

# Low energy capture of negatively charged kaons on light nuclei, the AMADEUS status and future physics case



Strange and non-strange mesons induced processes studies at  
DAFNE, J-PARC and RIKEN: present and future

10-11 July, LNF (INFN)

**Kristian Piscicchia\***

Laboratori Nazionali di Frascati (INFN)

Museo Storico della Fisica e Centro Studi e Ricerche Enrico Fermi

[kristian.piscicchia@lnf.infn.it](mailto:kristian.piscicchia@lnf.infn.it)

# Low-energy QCD in the u-d-s sector

$$\mathcal{L}_{eff} = \mathcal{L}_{mesons}(\Phi) + \mathcal{L}_B(\Phi, \Psi_B)$$

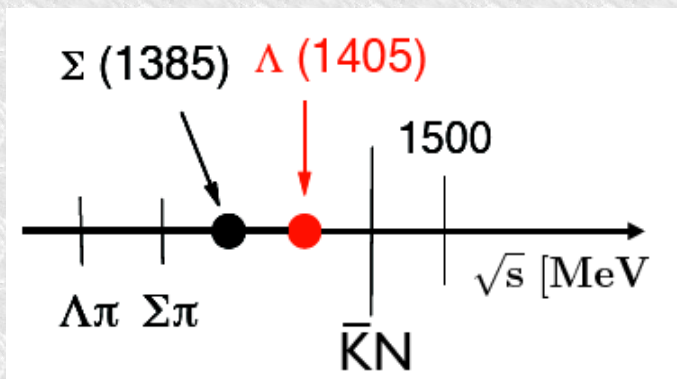
- Chiral perturbation theory: interacting systems of N-G bosons (pions, kaons) coupled to baryons works well for  $\pi\pi$ ,  $\pi N$ ,  $K^+N$  ..  
NOT for  $K^-N$  !!

- $K^- = (s\bar{u})$  strangeness = -1 ,  $K^+ = (\bar{u}s)$  strangeness = +1

strange baryons stable respect to strong interaction all have  $s = -1$

- the sub-threshold region is dominated by resonances  $\rightarrow$  complex multichannel dynamics

$\Lambda(1405)$  just below  $\bar{K}N$  threshold (1432 MeV)

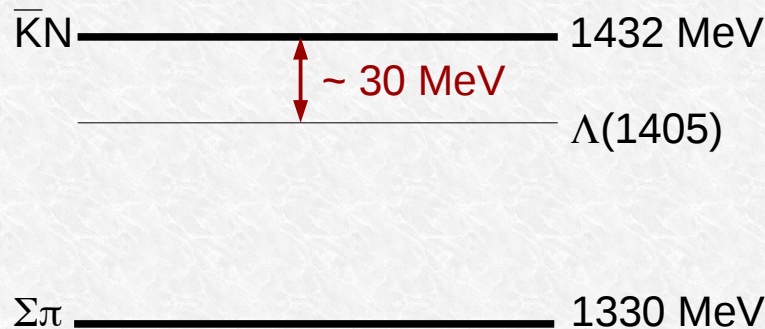


Possible solutions:

- Non-perturbative Coupled Channels approach: Chiral Unitary SU(3) Dynamics
- phenomenological  $\bar{K}N$  and NN potentials

# The $\Lambda(1405)$ case

**Mass** =  $1405.1^{+1.3}_{-1.0}$  MeV,  
**Width** =  $50.5 \pm 2.0$  MeV  
 $I = 0, S = -1, J^P = 1/2^-$ ,  
 Status: \*\*\*\*,  
 strong decay into  $\Sigma\pi$

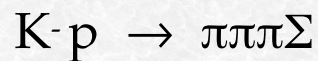


- 3 quark?
- **molecular?**
- **$\bar{K}N$  bound state?**
- pentaquark?

Theoretical prediction Dalitz-Tuan (1959)

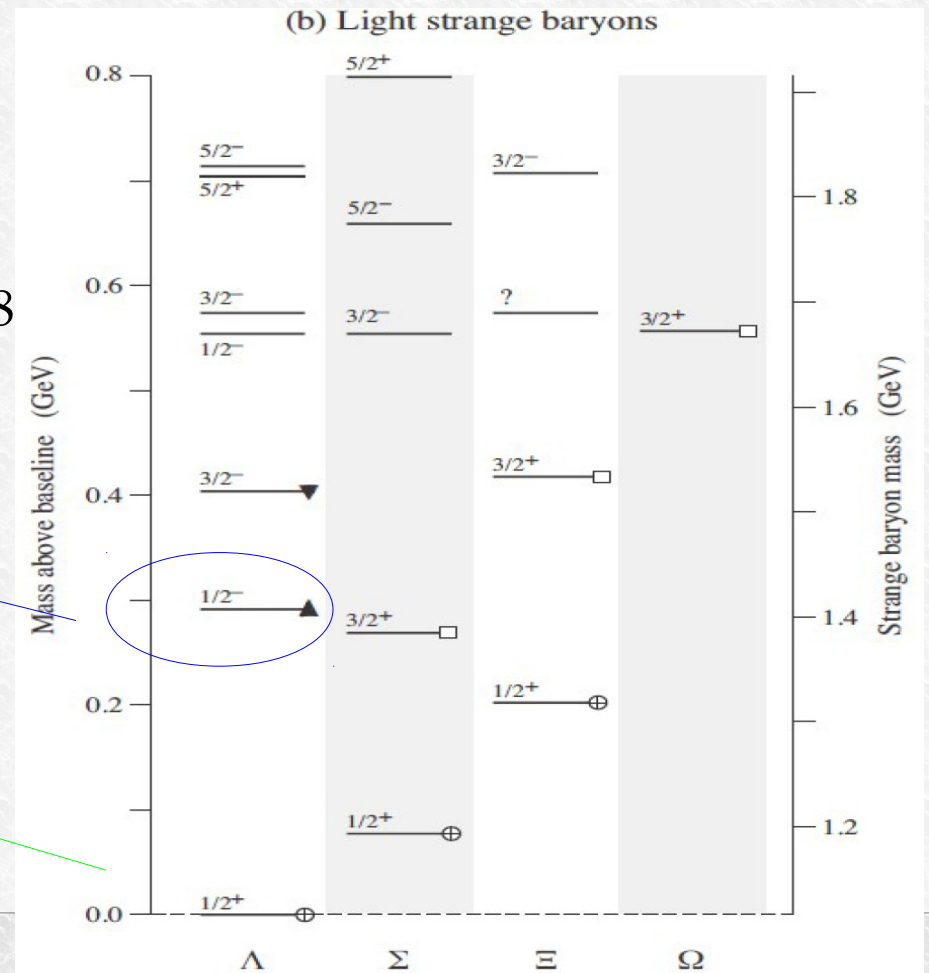
First experimental evidence:

M. H. Alston, et al., Phys. Rev. Lett. 6 (1961) 698



$\Lambda(1405)$

$\Lambda(1116)$



# The $\Lambda(1405)$ case

$\Lambda(1405)$  is located slightly below the  $\overline{KN}$  threshold (1432 MeV)

Three quark model picture difficulties to reproduce the  $\Lambda(1405)$ :

- According to its negative parity, one of the quarks has to be excited to  $l = 1$
- nucleon sector, we find the  $N(1535) \rightarrow$  the expected mass of the  $\Lambda^*$  is around 1700 MeV
- too big energy splitting observed between the  $\Lambda(1405)$  and the  $\Lambda(1520)$  interpreted as the spin-orbit partner ( $J^p = 3/2^-$ ).
- pentaquark ( $4q + qbar$  in  $l = 0$ ), but also predicts other, unobserved, excited baryons,

R. Dalitz and collaborators first suggested to interpret  $\Lambda(1405)$  as an  $\overline{KN}$  quasibound state.

R.H. Dalitz, T.C. Wong and G. Rajasekaran, Phys. Rev. **153** (1967) 1617.

# The $\Lambda(1405)$ case

BUBBLE CHAMBER search of the  $\Lambda(1405)$ :

- O. Braun et al. Nucl. Phys. B129 (1977) 1

K<sup>-</sup> induced reactions on d  $\rightarrow \Sigma^- \pi^+ n$  the resonance is found & 1420 MeV

- D. W. Thomas et al., Nucl. Phys. B56 (1973) 15

pion induced reaction  $\pi^- p \rightarrow K^+ \pi^- \Sigma$  the resonance is found & 1405 MeV

- R. J. Hemingway, Nucl. Phys. B253 (1985) 742

K<sup>-</sup> p  $\rightarrow \pi^- \Sigma^+(1660) \rightarrow \pi^- (\pi^+ \Lambda(1405)) \rightarrow \pi^- \pi^+ (\pi^- \Sigma)$  & 4.2 GeV

analysed by Dalitz and Deloff  $M = 1406.5 \pm 4.0$  MeV,  $\Gamma = 50 \pm 2$  MeV

# The $\Lambda(1405)$ case

THE “LINE-SHAPE” OF THE  $\Lambda(1405)$  DEPENDS ON THE OBSERVED CHANNEL !!

$$\frac{d\sigma(\Sigma^-\pi^+)}{dM} \propto \frac{1}{3} |T^0|^2 + \frac{1}{2} |T^1|^2 + \frac{2}{\sqrt{6}} \text{Re}(T^0 T^{1*})$$

$$\frac{d\sigma(\Sigma^+\pi^-)}{dM} \propto \frac{1}{3} |T^0|^2 + \frac{1}{2} |T^1|^2 - \frac{2}{\sqrt{6}} \text{Re}(T^0 T^{1*})$$

$$\frac{d\sigma(\Sigma^0\pi^0)}{dM} \propto \frac{1}{3} |T^0|^2$$

# The $\Lambda(1405)$ case

THE “LINE-SHAPE” OF THE  $\Lambda(1405)$  DEPENDS ON THE OBSERVED CHANNEL !!

$$\frac{d\sigma(\Sigma^-\pi^+)}{dM} \propto \frac{1}{3}|T^0|^2 + \frac{1}{2}|T^1|^2 + \frac{2}{\sqrt{6}}\text{Re}(T^0T^{1*})$$

$$\frac{d\sigma(\Sigma^+\pi^-)}{dM} \propto \frac{1}{3}|T^0|^2 + \frac{1}{2}|T^1|^2 - \frac{2}{\sqrt{6}}\text{Re}(T^0T^{1*})$$

$$\frac{d\sigma(\Sigma^0\pi^0)}{dM} \propto \frac{1}{3}|T^0|^2$$

IS DIFFERENT IN  $\Sigma^+\pi^-$  VS  $\Sigma^-\pi^+$

DUE TO ISOSPIN INTERFERENCE

# The $\Lambda(1405)$ case

THE “LINE-SHAPE” OF THE  $\Lambda(1405)$  DEPENDS ON THE OBSERVED CHANNEL !!

$$\frac{d\sigma(\Sigma^-\pi^+)}{dM} \propto \frac{1}{3}|T^0|^2 + \frac{1}{2}|T^1|^2 + \frac{2}{\sqrt{6}}\text{Re}(T^0T^{1*})$$

$$\frac{d\sigma(\Sigma^+\pi^-)}{dM} \propto \frac{1}{3}|T^0|^2 + \frac{1}{2}|T^1|^2 - \frac{2}{\sqrt{6}}\text{Re}(T^0T^{1*})$$

$$\frac{d\sigma(\Sigma^0\pi^0)}{dM} \propto \frac{1}{3}|T^0|^2$$

IS DIFFERENT IN  $\Sigma^+\pi^-$  VS  $\Sigma^-\pi^+$   
DUE TO ISOSPIN INTERFERENCE

THE CLEANEST SIGNATURE OF THE  $\Lambda(1405)$  IS GIVEN BY THE NEUTRAL CHANNEL:

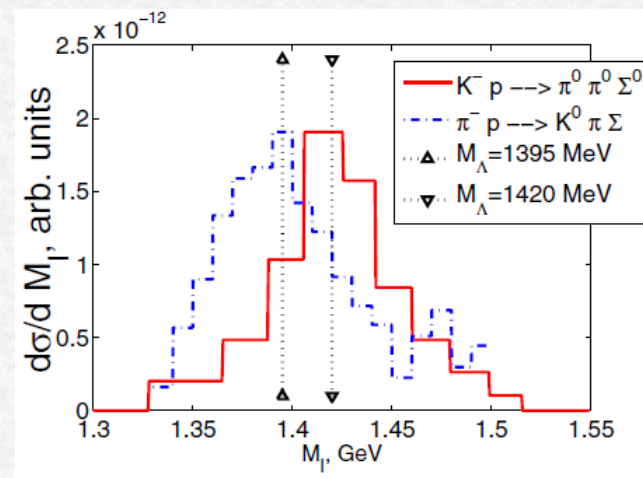
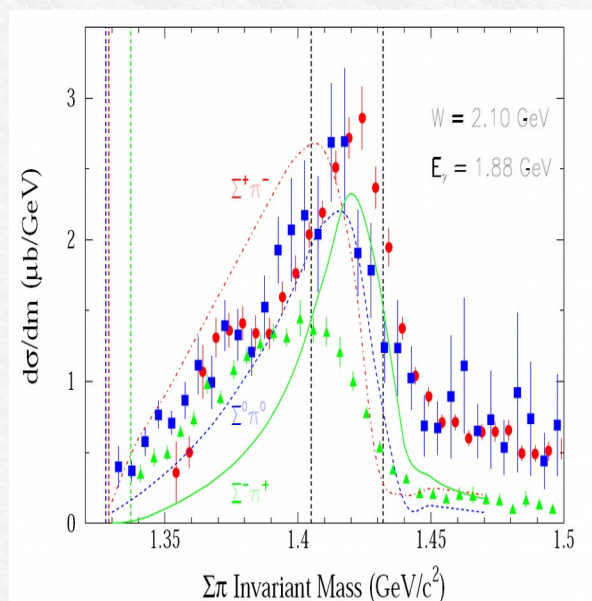
- is free from isospin interference
- is purely  $I = 0$ , no  $\Sigma(1385)$  contamination.



# $\Lambda(1405)$ .. the golden channel

Crystall Ball:  $K^- p \rightarrow \Sigma^0 \pi^0 \pi^0$  for kaon momentum in the range (514-750 MeV/c). S. Prakhov et al. Phys Rev. C70 (2004) 03465

(interpreted by Magas et al. PRL 95, 052301 (2005))



CLAS:  $\gamma p \rightarrow K^+ \Sigma \pi$

AIP Conf.Proc. 1441 (2012) 296-298

COSY julich:  $pp \rightarrow pK^+ \Sigma^0 \pi^0$

(I. Zychor et al., Phys. Lett. B 660 (2008) 167)

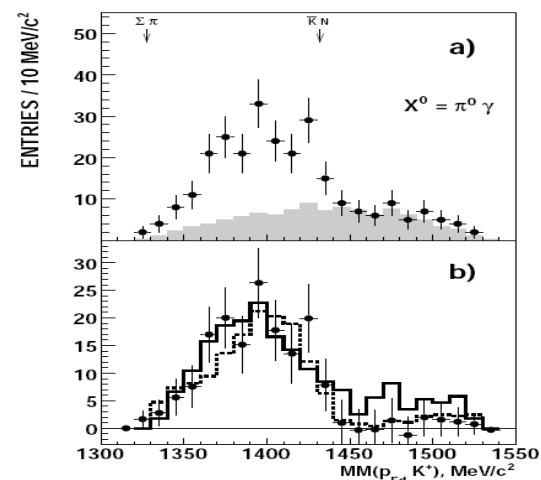
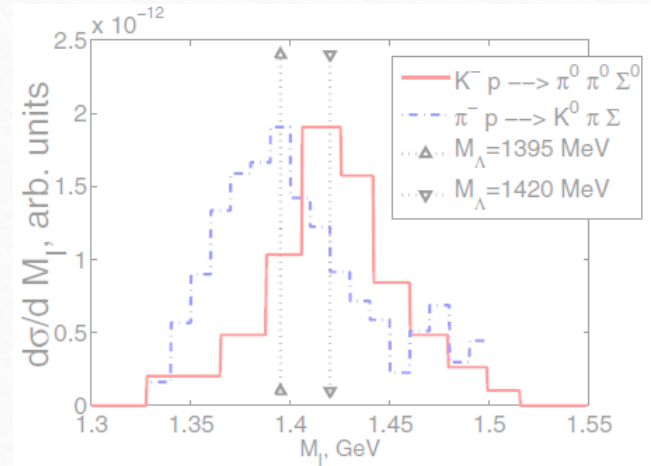


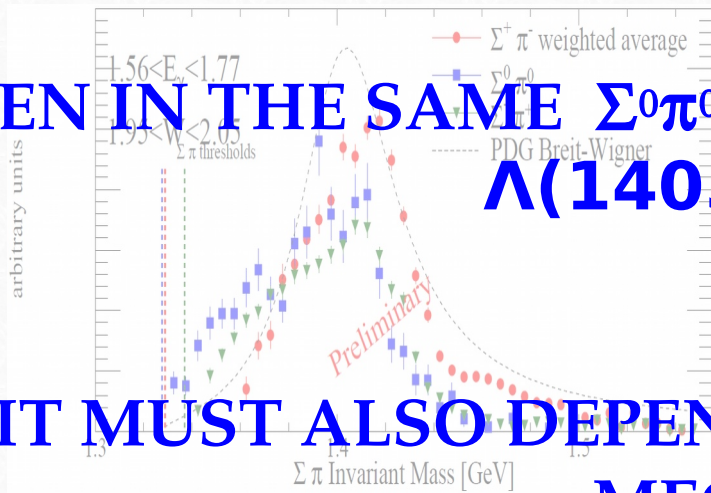
Fig. 4. a) Missing-mass  $MM(p_{Fd}K^+)$  distribution for the  $pp \rightarrow pK^+ p\pi^- X^0$  reaction for events with  $M(p_{sd}\pi^-) \approx m(\Lambda)$  and  $MM(pK^+ p\pi^-) > 190 \text{ MeV}/c^2$ . Exper-

# $\Lambda(1405)$ .. the golden channel

Crystall Ball:  $K^- p \rightarrow \Sigma^0 \pi^0 \pi^0$  for kaon momentum in the range (514-750 MeV/c). S. Prakhov et al. Phys Rev. C70 (2004) 03465 (Magas et al. PRL 95, 052301 (2005))



**EVEN IN THE SAME  $\Sigma^0 \pi^0$  THE "LINE-SHAPE" OF THE  $\Lambda(1405)$  CHANGES**



CLAS  $\gamma p \rightarrow p K^+ \Sigma \pi$

AIP Conf.Proc. 1441 (2012) 296-298

**IT MUST ALSO DEPEND ON THE PRODUCTION MECHANISM**

COSY julich:  $pp \rightarrow p K^+ \Sigma^0 \pi^0$   
( I. Zychor et al., Phys. Lett. B 660 (2008) 167 )

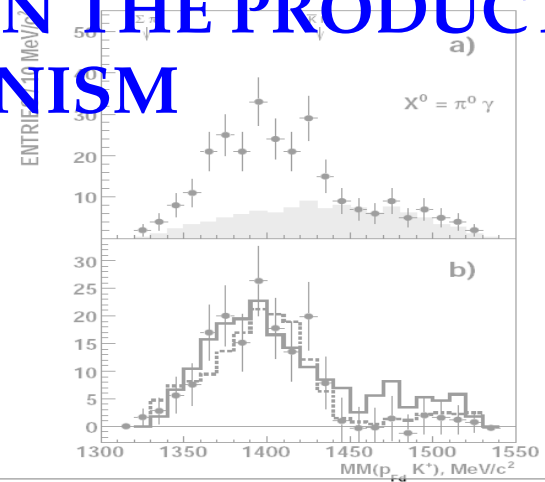


Fig. 4. a) Missing-mass  $MM(p_{sd} \pi^-)$  distribution for the  $pp \rightarrow p K^+ p \pi^- X^0$  reaction for events with  $M(p_{sd} \pi^-) \approx m(\Lambda)$  and  $MM(p_{K^+} \pi^-) > 190 \text{ MeV}/c^2$ . Exper-

# The $\Lambda(1405)$ case

- Chiral unitary models:  $\Lambda(1405)$  is an  $I = 0$  quasibound state emerging from the coupling between the  $\bar{K}N$  and the  $\Sigma\pi$  channels. Two poles in the neighborhood of the  $\Lambda(1405)$ :

*two poles*: about 1420 ; about = 1380 MeV

Phys. Lett. B 500 (2001), Phys. Rev. C 66 (2002), (Nucl. Phys. A 725(2003) 181) .. many others .. (Nucl. Phys. A881, 98 (2012)) .. others

mainly coupled to  $\bar{K}N$

mainly coupled to  $\Sigma\pi$

→ line-shape depends on production mechanism

- Akaishi-Esmaili-Yamazaki phenomenological potential

Phys. Lett. B 686 (2010) 23-28 Confirmation of single pole ansatz?

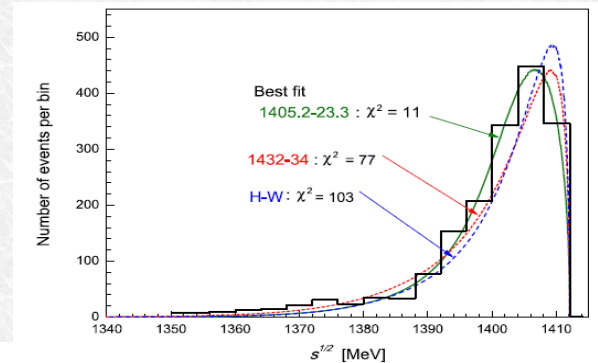
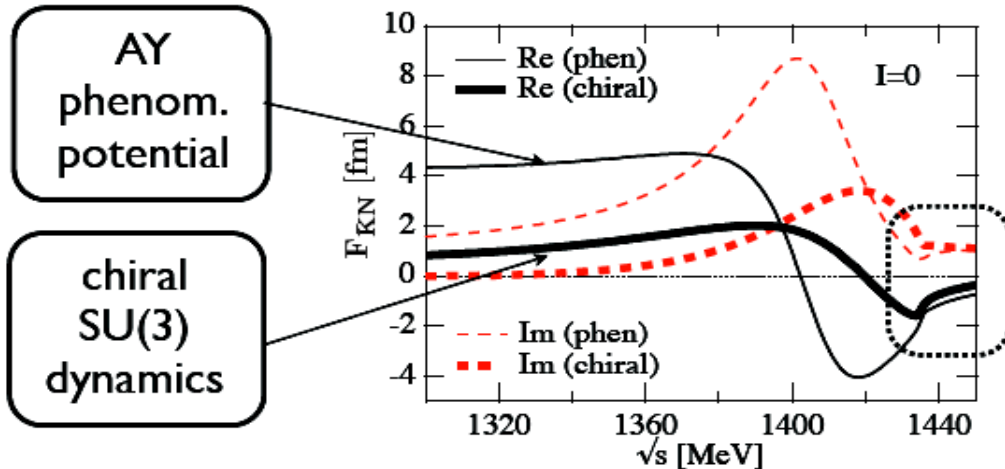
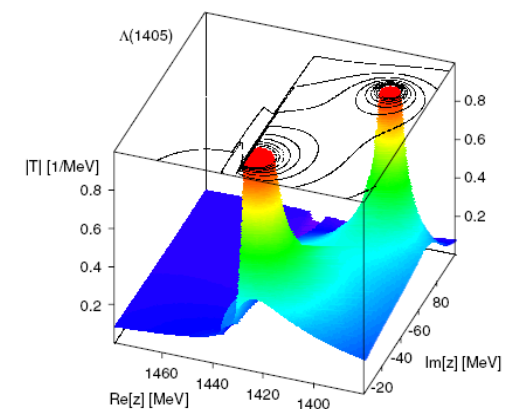


Fig. 6. Detailed differences in  $M_{\Sigma\pi}$  spectra among the Hyodo-Weise prediction and the present model predictions.



large differences in subthreshold extrapolations



- Chiral dynamics predicts significantly weaker attraction than AY (local, energy independent) potential in far-subthreshold region

# The $\Lambda(1405)$ case

Two main **biases**:

- the **kinematical energy threshold 1412 MeV**  
( $M_K + M_p - |BE_p|$ ) the high pole energy region is closed,
- The **shape and the amplitude of the NON-RESONANT  $\Sigma\pi$  production** below  $K\bar{p}N$  threshold is unknown.

An ideal experiment:

- $\Lambda(1405)$  is produced in  $K^- p$  absorption  $\rightarrow$  mainly coupled to the high mass pole,
- $\Lambda(1405)$  is observed in the  $\Sigma^0\pi^0$  decay channel (pure isospin 0),
- $K^-$  is absorbed in-flight on a bound proton with  $p_K \sim 100$  MeV,  $\Sigma\pi$  invariant mass gain of  $\sim 10$  MeV to open an energy window to the high mass pole.
- Knowledge of the  $\Sigma\pi$  NON-RESONANT production amplitude.

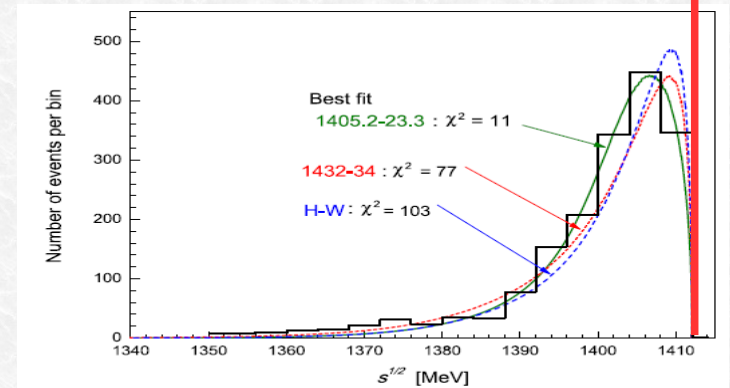
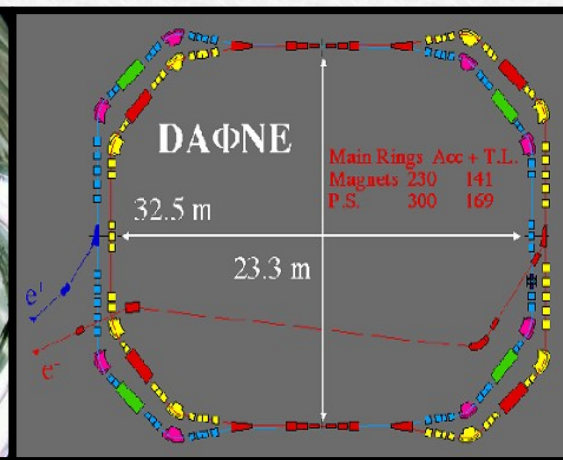
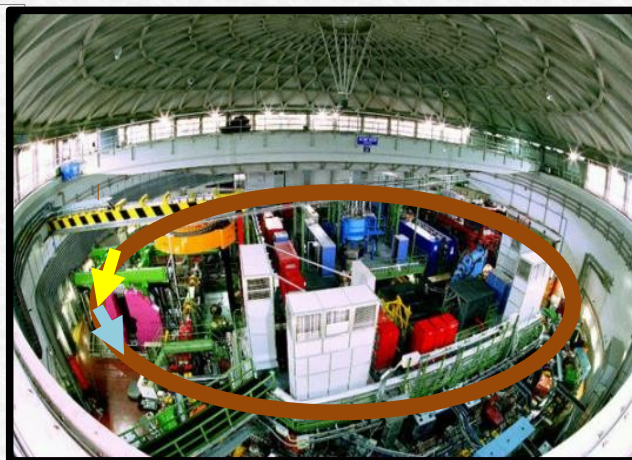


Fig. 6. Detailed differences in  $M_{\Sigma\pi}$  spectra among the Hyodo-Weise prediction and the present model predictions.

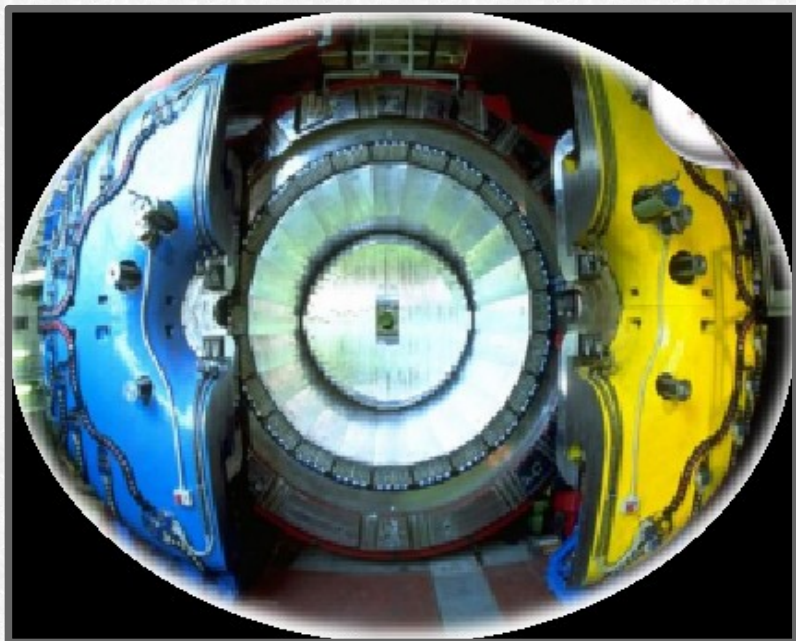
# AMADEUS & DAΦNE

## DAΦNE

- double ring  $e^+e^-$  collider working at C.M. energy of  $\phi$ , producing  $\approx 1000 \phi /s$ 
  - $\phi \rightarrow K^+K^-$  (BR =  $(49.2 \pm 0.6)\%$ )
    - **low momentum** Kaons  $\approx 127 \text{ Mev}/c$
  - **back to back**  $K^+K^-$  topology



**AMADEUS step 0**  $\rightarrow$  KLOE 2004-2005 dataset analysis ( $\mathcal{L} = 1.74 \text{ pb}^{-1}$ )



## KLOE

- Cylindrical drift chamber with a  **$4\pi$  geometry** and electromagnetic calorimeter
  - **96% acceptance**
- optimized in the energy range of all **charged particles** involved
- **good performance** in detecting **photons and neutrons** checked by kloNe group

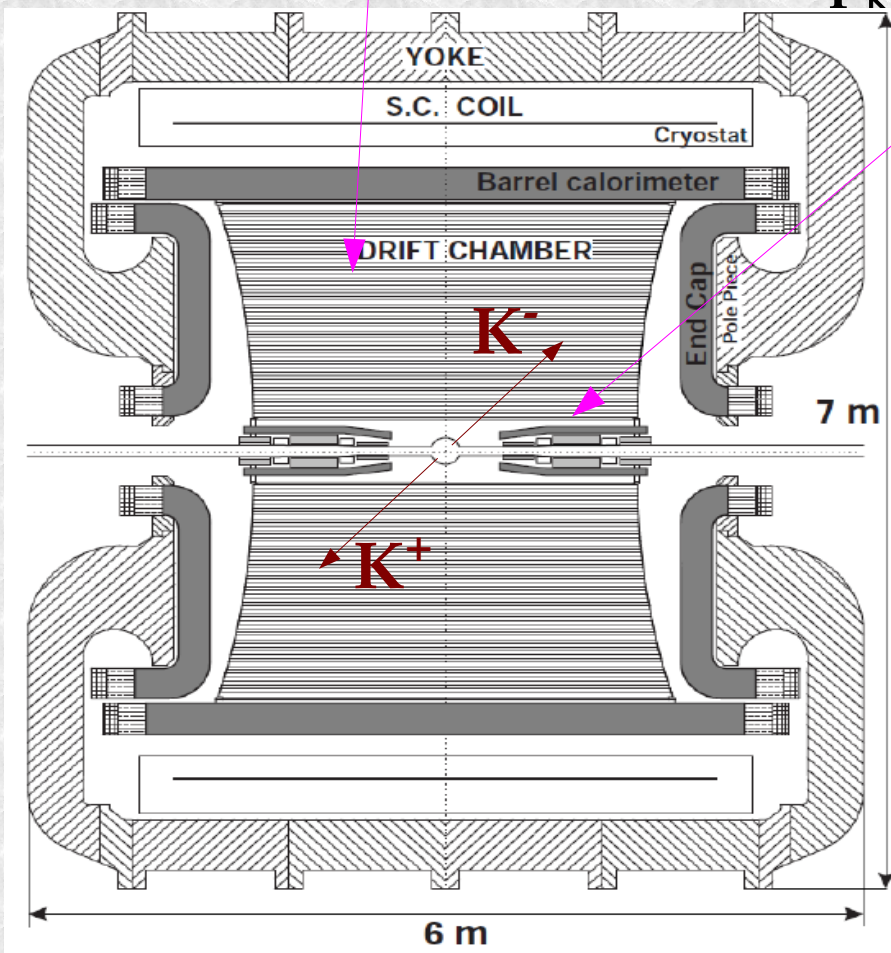
[M. Anelli et al., Nucl Inst. Meth. A 581, 368 (2007)]

# K<sup>-</sup> absorption on light nuclei

from the materials of the KLOE detector

DC gas (90% He, 10% C<sub>4</sub>H<sub>10</sub>) & DC wall (C + H)

AT-REST (K<sup>-</sup> absorbed from atomic orbit) or IN-FLIGHT  
(p<sub>K</sub> ~ 100 MeV)



Advantage:

**excellent resolution ..**

$$\sigma_{p\Lambda} = 0.49 \pm 0.01 \text{ MeV}/c \text{ in DC gas}$$

$$\sigma_{m_{\gamma\gamma}} = 18.3 \pm 0.6 \text{ MeV}/c^2$$

Disadvantage:

Not dedicated target → **different nuclei contamination** → complex interpretation .. but  
→ **new features .. K<sup>-</sup> in flight absorption.**

# The scientific goal of AMADEUS

Low energy QCD in strangeness sector is still waiting for experimental conclusive constrains on:

1)  $\bar{K}$ -N potential → how deep can an antikaon be bound in a nucleus?

-  $U_{KN}$  strongly affects the position of the  $\Lambda(1405)$  state → we investigate it through  $(\Sigma-\pi)^0$  decay ---  $Y \pi$  CORRELATION

- if  $U_{KN}$  is strongly attractive then  $K^-$  NN bound states should appear → we investigate through  $(\Lambda/\Sigma-N)$  decay ---  $Y N$  CORRELATION

2)  $Y$ -N potential → extremely poor experimental information from scattering data

-  $U_{YN}$  determines the strength of the final state  $YN$  (elastic & inelastic) scattering in nuclear environment → could be tested by  $Y N$  CORRELATION

# The scientific goal of AMADEUS

Low energy QCD in strangeness sector is still waiting for experimental conclusive constrains on:

1)  $\bar{K}$ -N potential → how deep can an antikaon be bound in a nucleus?

-  $U_{KN}$  strongly affects the position of the  $\Lambda(1405)$  state → we investigate it through  $(\Sigma-\pi)^0$  decay ---  $\Upsilon \pi$  CORRELATION

- if  $U_{KN}$  is strongly attractive then  $K^-$  NN bound states should appear → we investigate through  $(\Lambda/\Sigma-N)$  decay ---  $\Upsilon N$  CORRELATION

2)  $\Upsilon$ -N potential → extremely poor experimental information from scattering data

-  $U_{YN}$  determines the strength of the final state  $\Upsilon N$  (elastic & inelastic) scattering in nuclear environment → could be tested by  $\Upsilon N$  CORRELATION



**K<sup>-</sup> - N single nucleon absorption  
the case of the  $\Lambda(1405)$**

# $\Lambda(1405)$ case

Phys.Rev.Lett.95:052301,2005

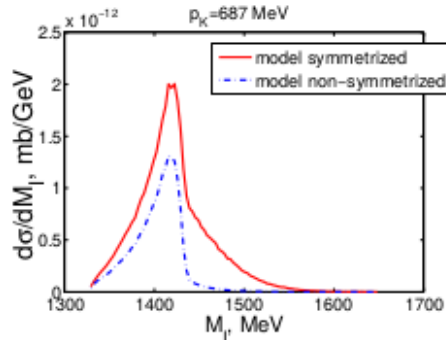


FIG. 4: Theoretical ( $\pi^0\Sigma^0$ ) invariant mass distribution for an initial kaon lab momenta of 687 MeV. The non-symmetrized distribution also contains the factor 1/2 in the cross section.

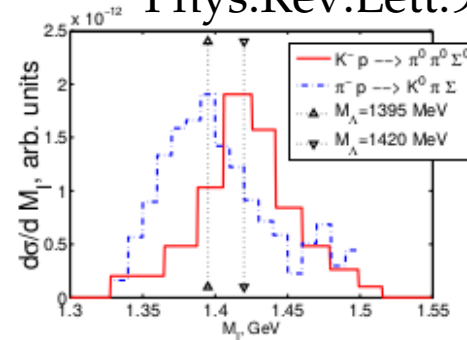
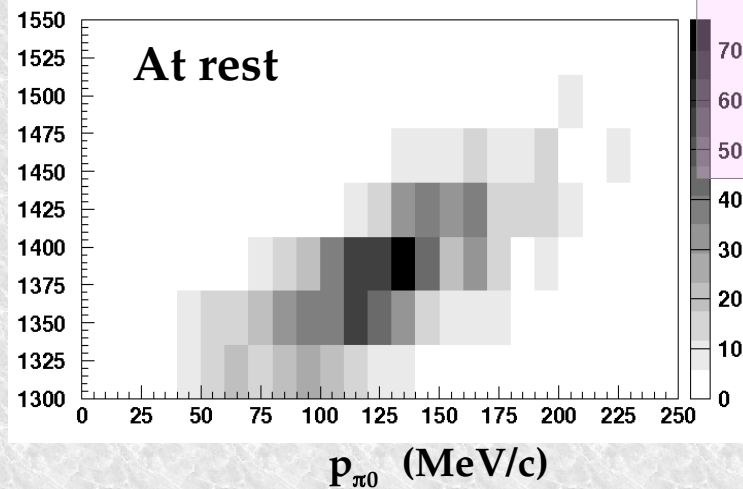
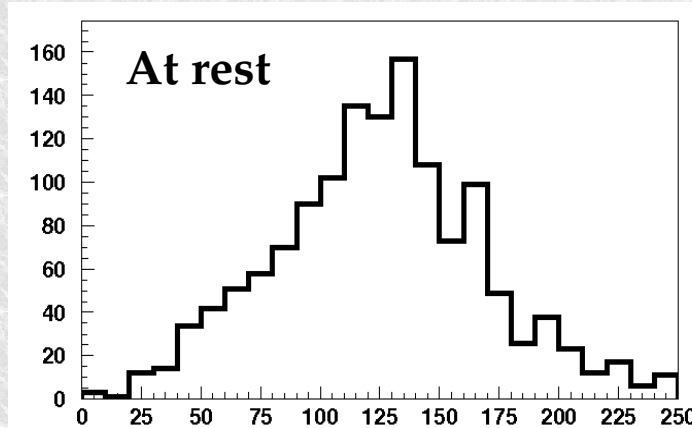
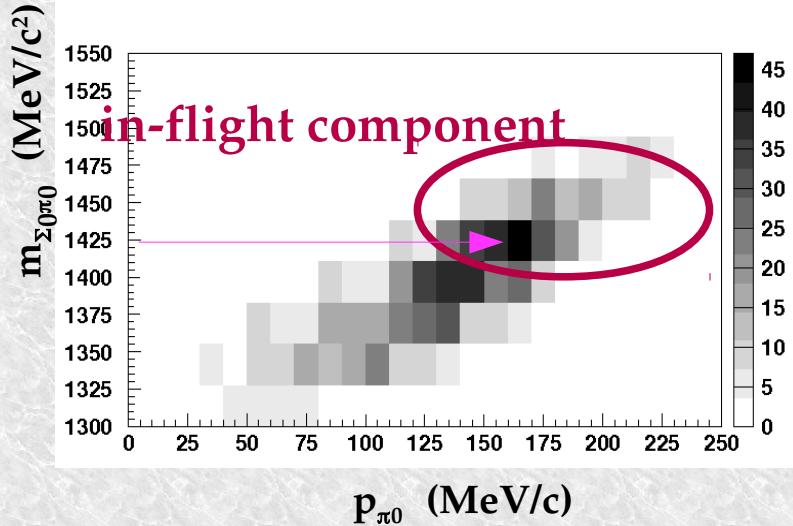
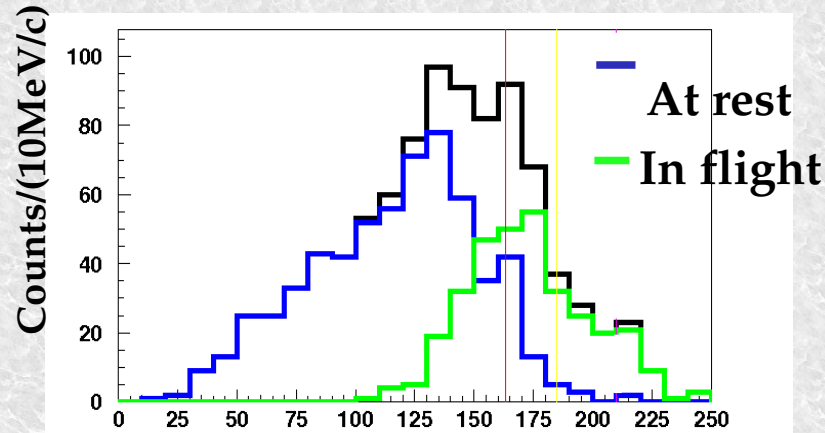


FIG. 5: Two experimental shapes of  $\Lambda(1405)$  resonance. See text for more details.

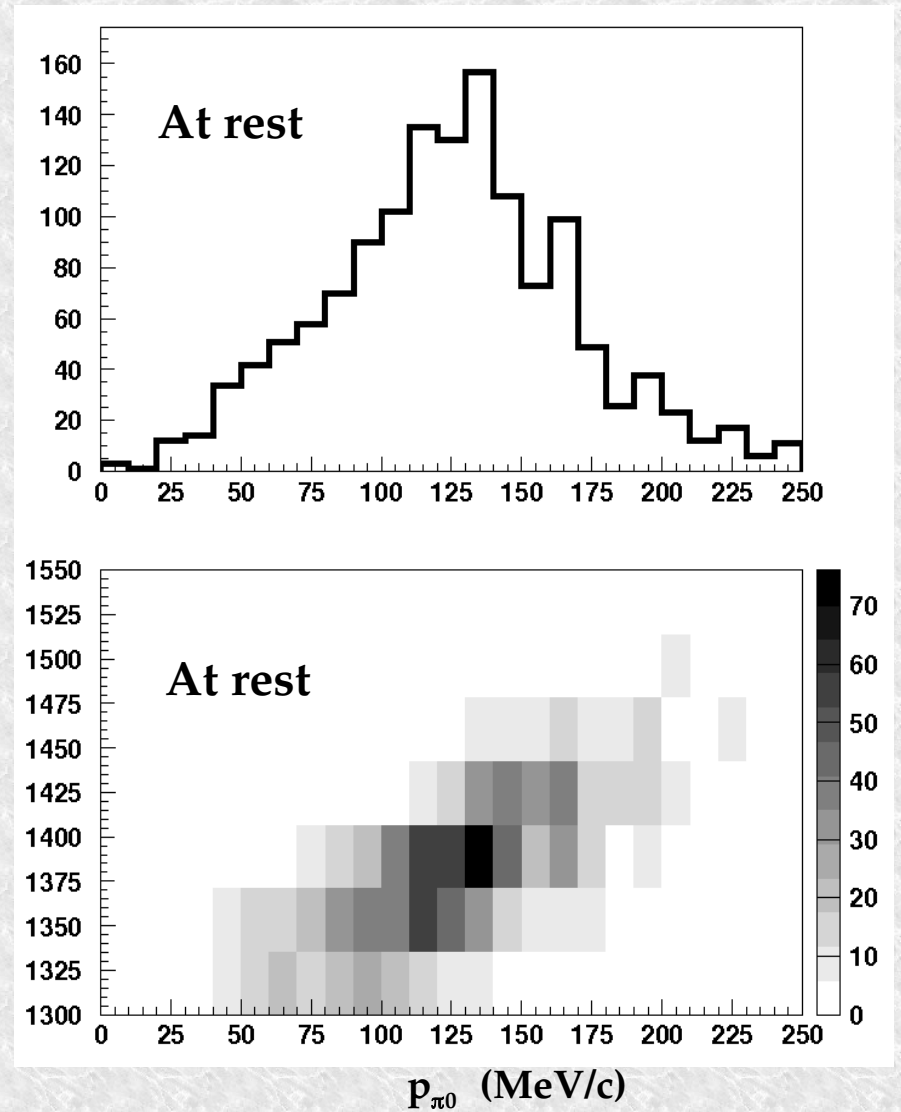
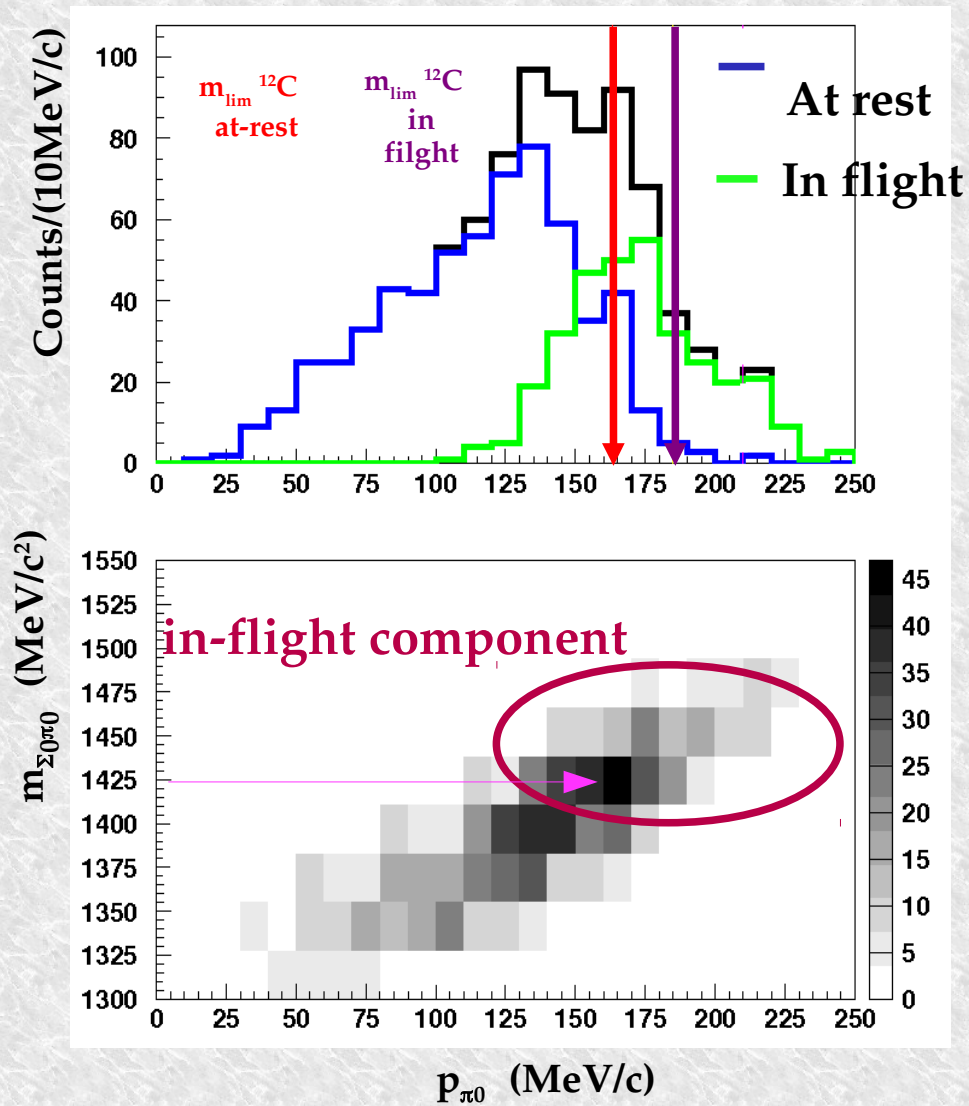
$p_{\pi^0}$  resolution:  $\sigma_p \approx 12 \text{ MeV}/c$



IN-FLIGHT  
K-12C  
opens a window  
between 1416 MeV  
and K-Nth

# Complex interpretation due to K- H absorptions ongoing

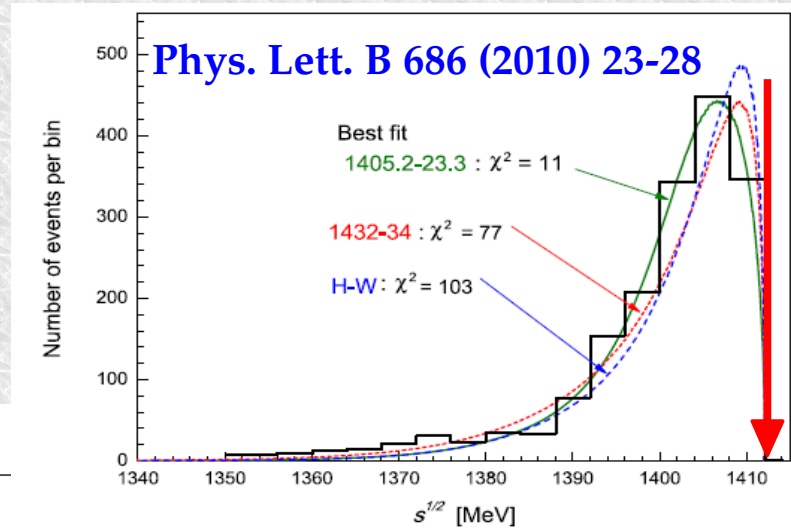
$p_{\pi 0}$  resolution:  $\sigma_p \approx 12 \text{ MeV}/c$



# $\Sigma^+ \pi^-$ correlation

$K^- p \rightarrow \Sigma^+ \pi^-$  detected via:  $(p\pi^0) \pi^-$

Possibility to disentangle: **Hydrogen**, **in-flight**, **at-rest**,  $K^-$  capture



$p_{\pi^-}$  resolution:  $\sigma_p \approx 1$  MeV/c

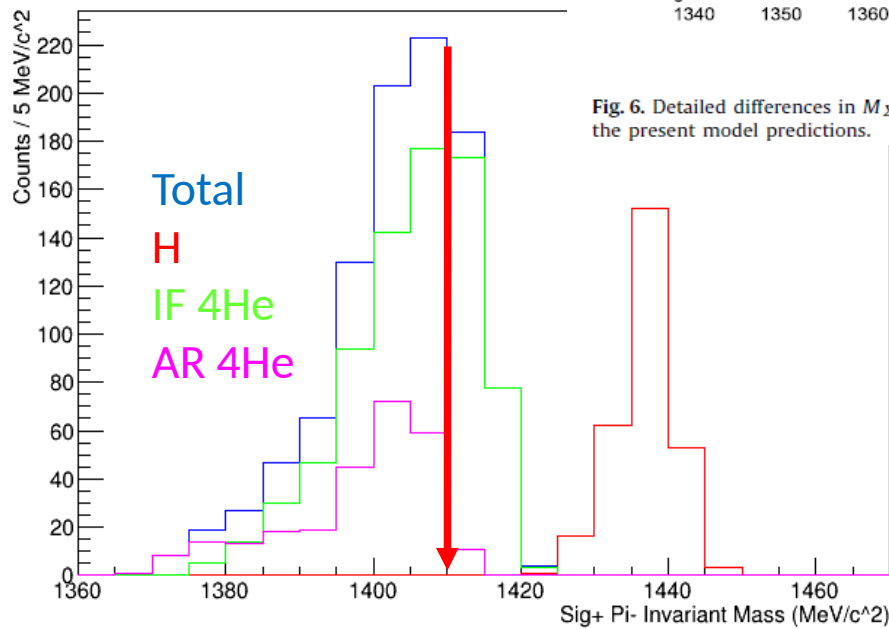
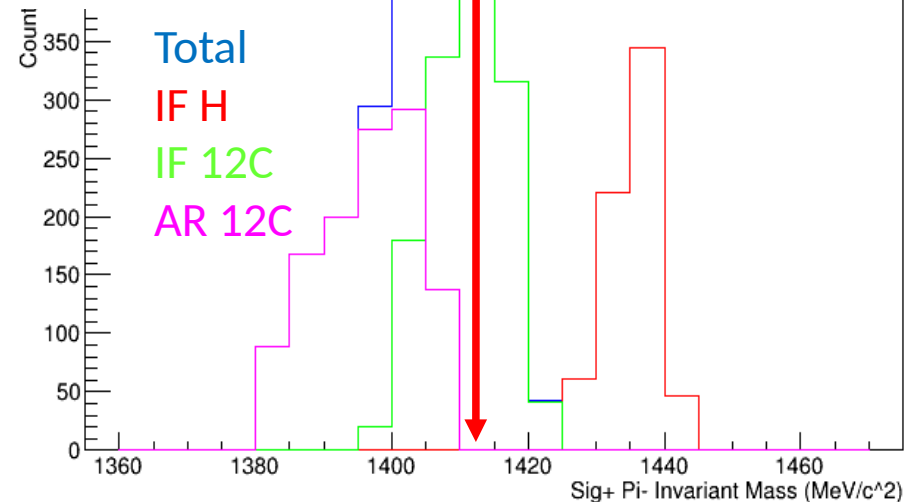


Fig. 6. Detailed differences in  $M_{\Sigma\pi}$  spectra among the Hyodo-Weise prediction and the present model predictions.



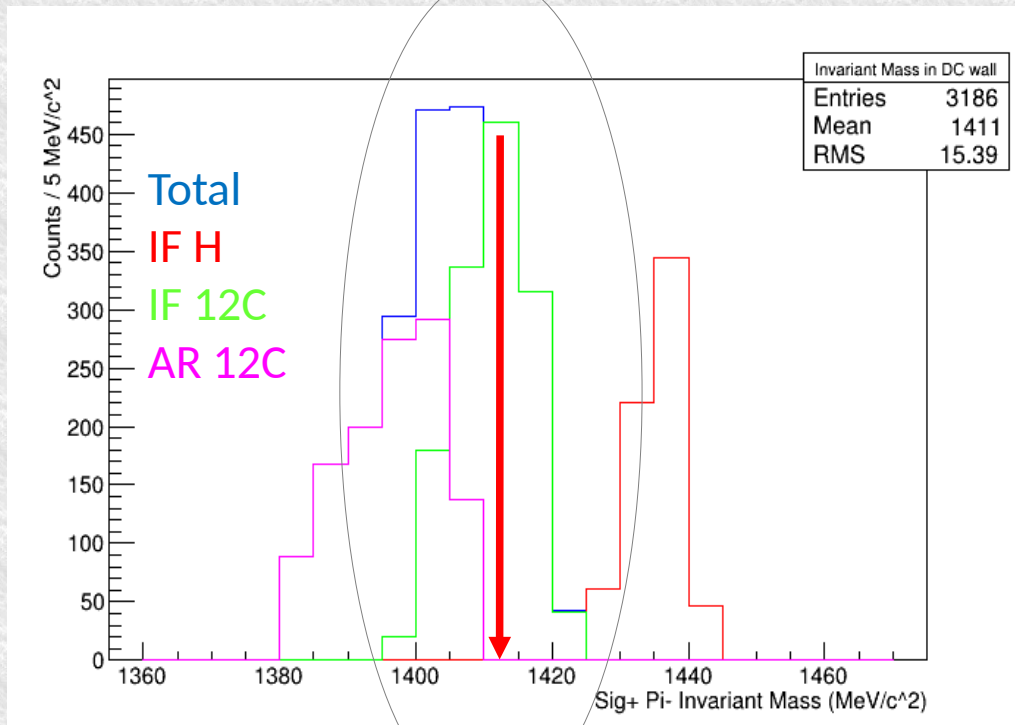
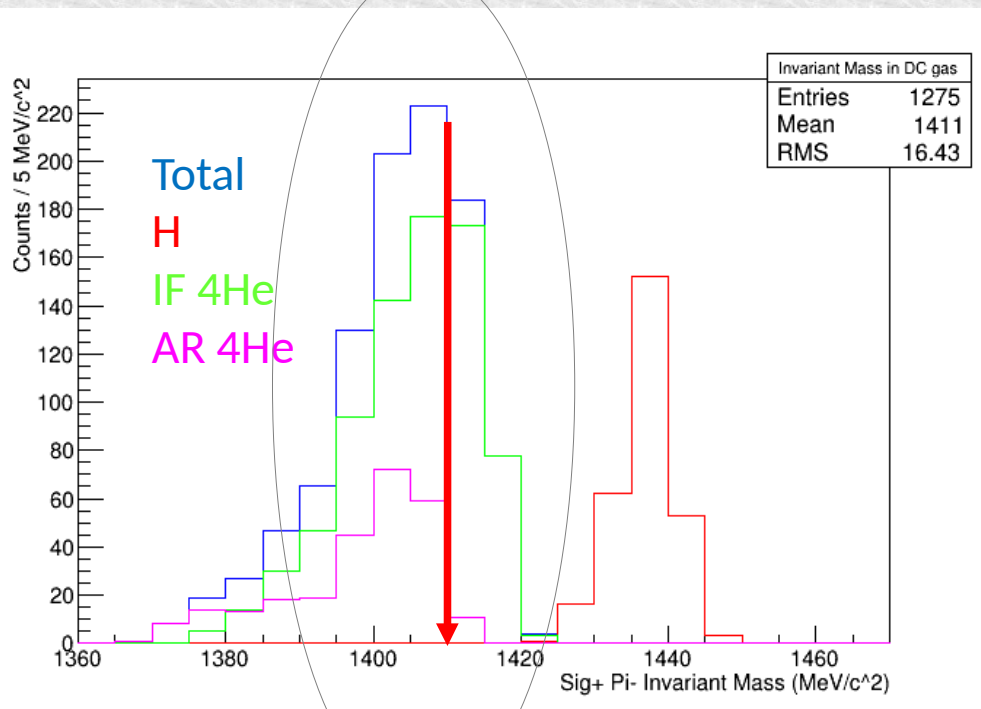
Invariant Mass in DC wall	
Entries	3186
Mean	1411
RMS	15.39

# $\Sigma^+\pi^-$ correlation

$K^-p \rightarrow \Sigma^+\pi^-$  detected via:  $(p\pi^0)\pi^-$

Possibility to disentangle: Hydrogen, in-flight, at-rest,  $K^-$  capture

if resonant production contribution is important a high mass component appears!



# Resonant VS non-resonant

$$K^- N \rightarrow (Y^* ?) \rightarrow Y \pi$$

in medium, how much comes from resonance ?

Non resonant transition amplitude:

- Never measured before below threshold  
(33 MeV below threshold):

$$E_{K_n} = -|B_n| - \frac{p_3^2}{2\mu_{\pi, \Lambda, 3He}},$$

- few, old theoretical calculations  
(Nucl. Phys. B179 (1981) 33-48)

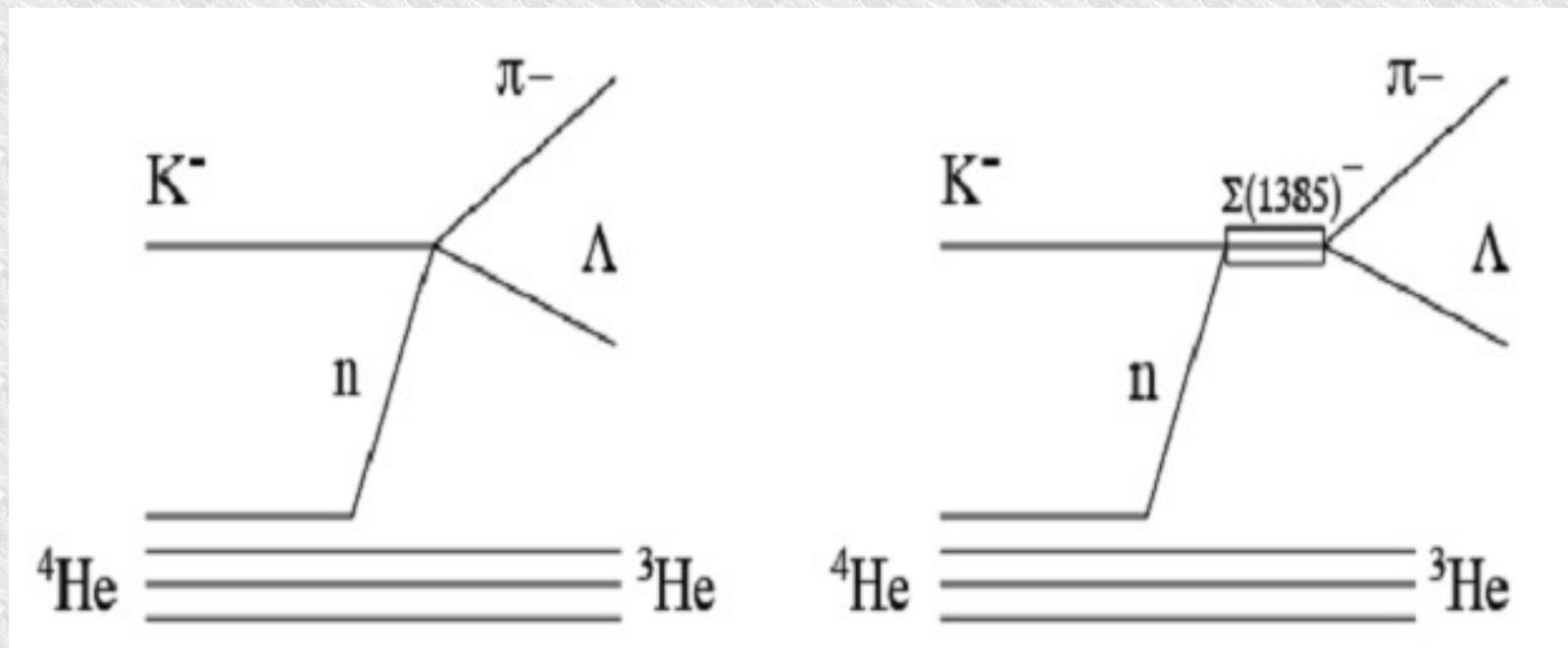
# Resonant VS non-resonant

Investigated using:

$K^- "n" \rightarrow \Lambda \pi^-$  direct formation in  ${}^4\text{He}$

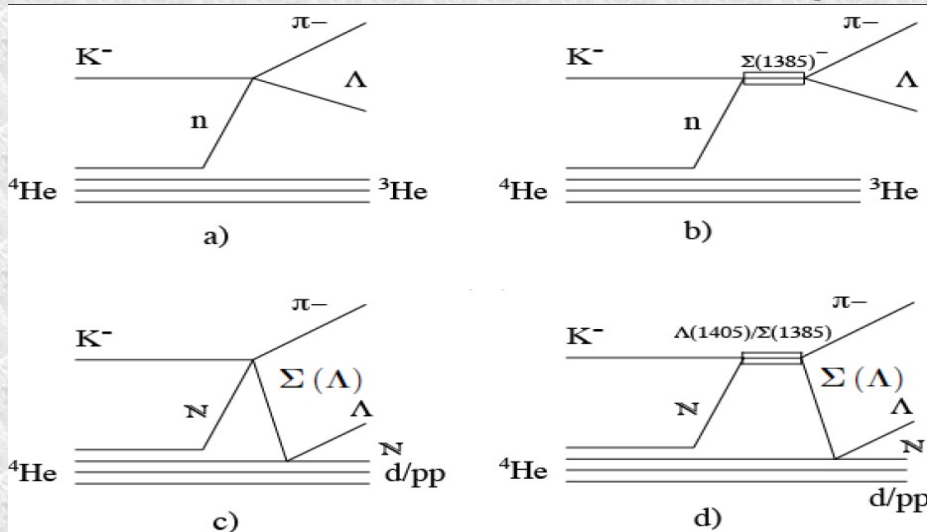
the goal is to measure  $|f^{N-R}_{\Lambda\pi}(\mathbf{I}=1)|$

to get information on  $|f^{N-R}_{\Sigma\pi}(\mathbf{I}=0)|$



# $K^- \ ^4\text{He} \rightarrow \Lambda p^- \ ^3\text{He}$ resonant and non-resonant processes

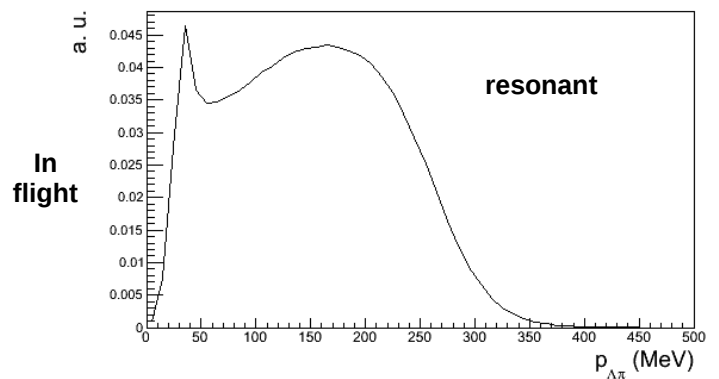
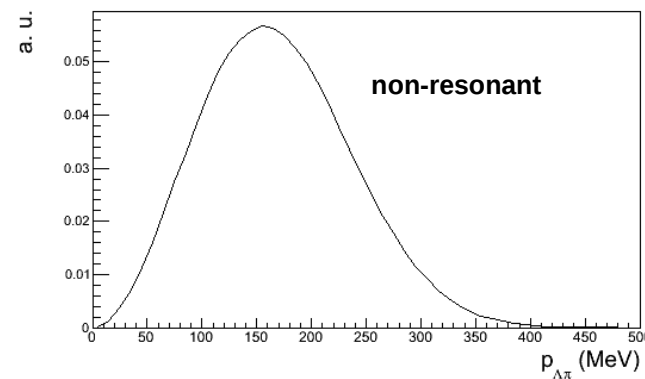
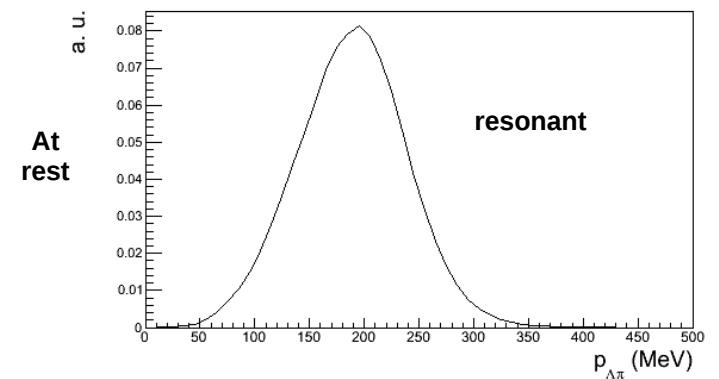
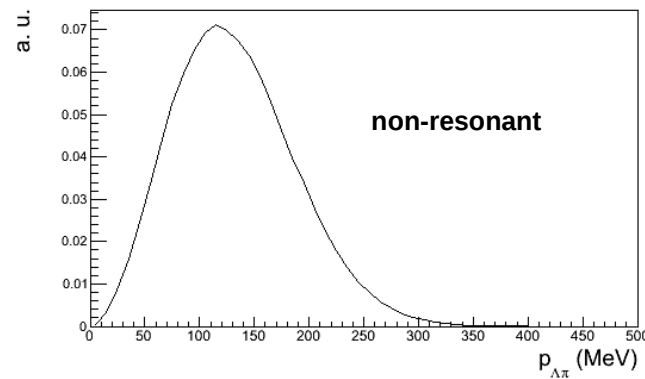
## Nucl. Phys. A954 (2016) 75-93



Theoretical shapes for :

total  $\Lambda\pi^-$  momentum spectra for the resonant ( $\Sigma^*$ ) and non-resonant ( $l = 1$ ) processes were calculated, for both S-state and P-state  $K^-$  capture at-rest and in-flight. Corrections to the amplitudes due to  $\Lambda/\pi$  final state interactions were estimated.

Collaboration with  
S. Wycech





# How to extract the $K^- n \rightarrow \Lambda \pi^-$ non resonant transition amplitude

simultaneous fit ( $p_{\Lambda\pi^-} - m_{\Lambda\pi^-} - \cos(\theta_{\Lambda\pi^-})$ ) with signal  and background  processes :

- non resonant  $K^-$  capture at-rest from  $S$  states in  ${}^4\text{He}$
- resonant  $K^-$  capture at-rest from  $S$  states in  ${}^4\text{He}$
- non resonant  $K^-$  capture in-flight in  ${}^4\text{He}$
- resonant  $K^-$  capture in-flight in  ${}^4\text{He}$

- primary  $\Sigma\pi^-$  production followed by the  $\Sigma N \rightarrow \Lambda N'$  conversion process
- $K^-$  capture processes in  ${}^{12}\text{C}$  giving rise to  $\Lambda\pi^-$  in the final state

**In order to extract:**

**NR-ar/RES-ar**

**&**

**NR-if/RES-if**

# Results for the $K^- n \rightarrow \Lambda \pi^-$ non resonant transition amplitude

Channels	Ratio/Amplitude	$\sigma_{\text{stat}}$	$\sigma_{\text{syst}}$
RES-ar/NR-ar	0.39	$\pm 0.04$	$+0.18$ $-0.07$
RES-if/NR-if	0.23	$\pm 0.03$	$+0.23$ $-0.22$
NR-ar	12.00 %	$\pm 1.66$ %	$+1.96$ % $-2.77$ %
NR-if	19.24 %	$\pm 4.38$ %	$+5.90$ % $-3.33$ %
$\Sigma \rightarrow \Lambda$ conv.	2.16 %	$\pm 0.30$ %	$+1.62$ % $-0.83$ %
$K^- {}^{12}\text{C}$ capture	57.00 %	$\pm 1.23$ %	$+2.21$ % $-3.19$ %

Preliminary

TABLE I. Resonant to non-resonant ratios and amplitude of the different channels extracted from the fit of the  $\Lambda \pi^-$  sample. The statistical and systematic errors are also shown. See text for details.

extracted:  
**NR-ar/RES-ar**      &      **NR-if/RES-if**

# Simultaneous momentum – angle – mass fit

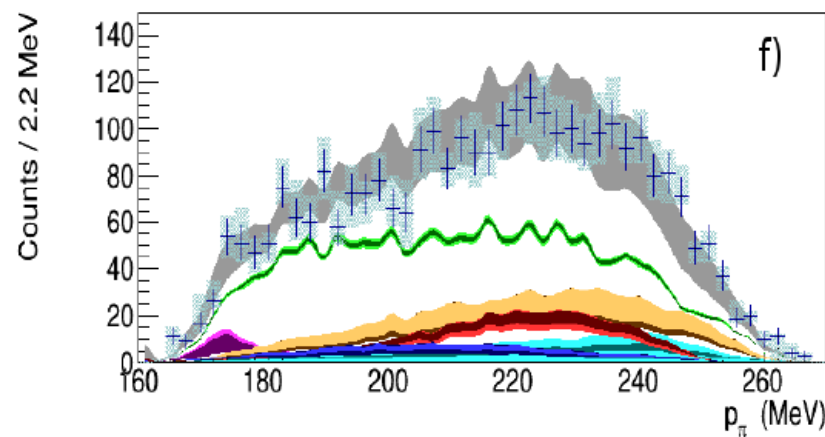
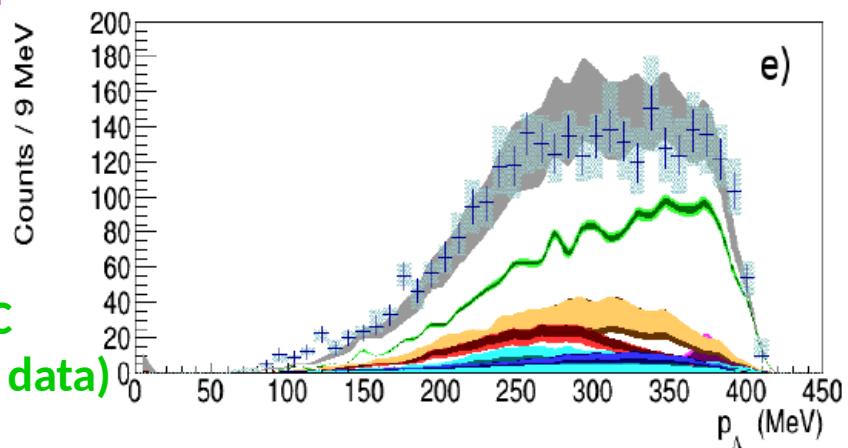
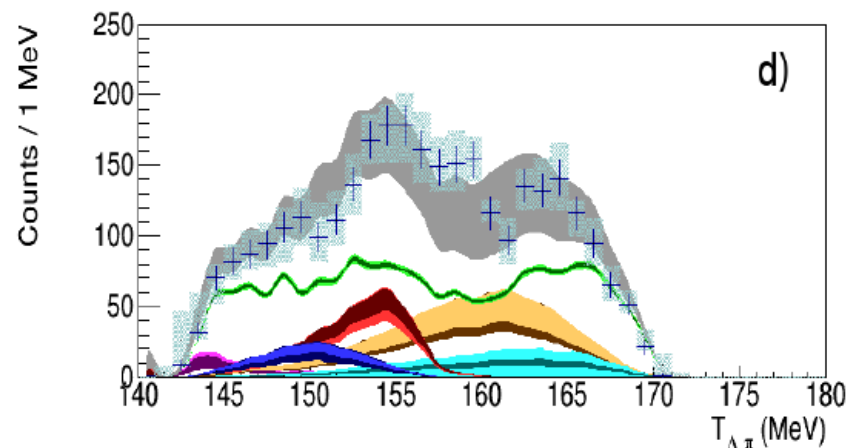
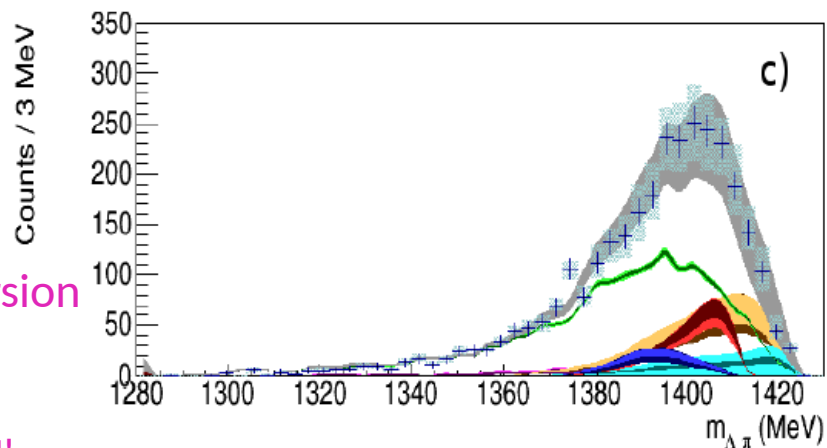
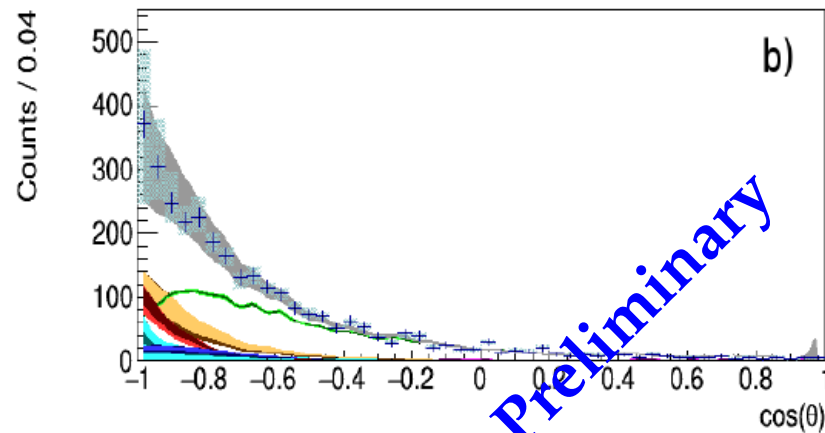
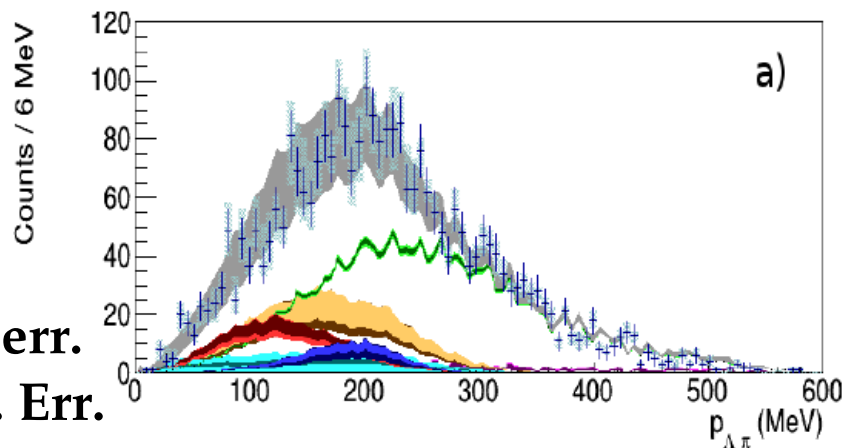
Light band sys err.  
Dark band stat. Err.

$\Sigma/\Lambda$  nuclear conversion

$K-N \rightarrow \Sigma \pi$

$\rightarrow \Sigma N \rightarrow \Lambda N'$

Absorptions in  $^{12}\text{C}$   
(from Carbon wall data)

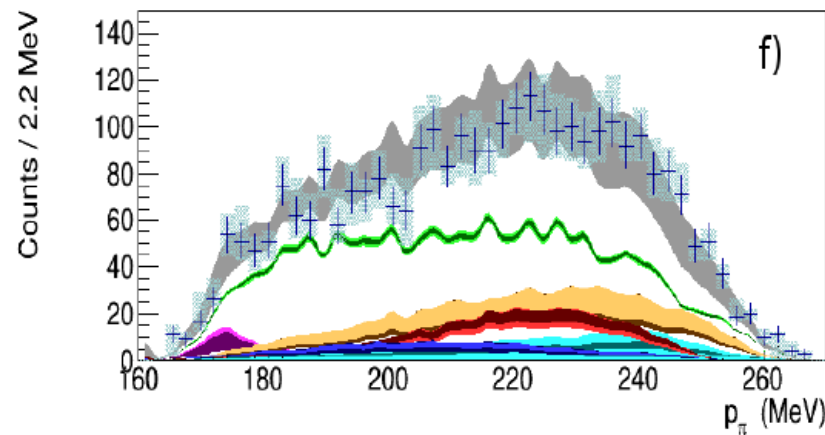
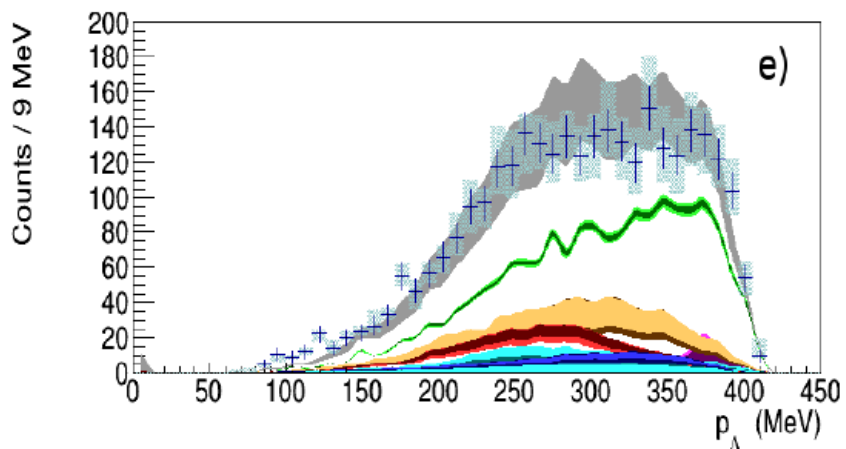
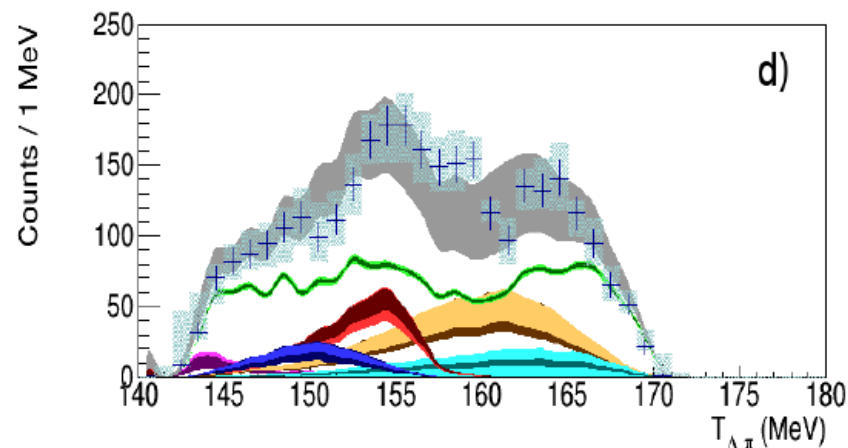
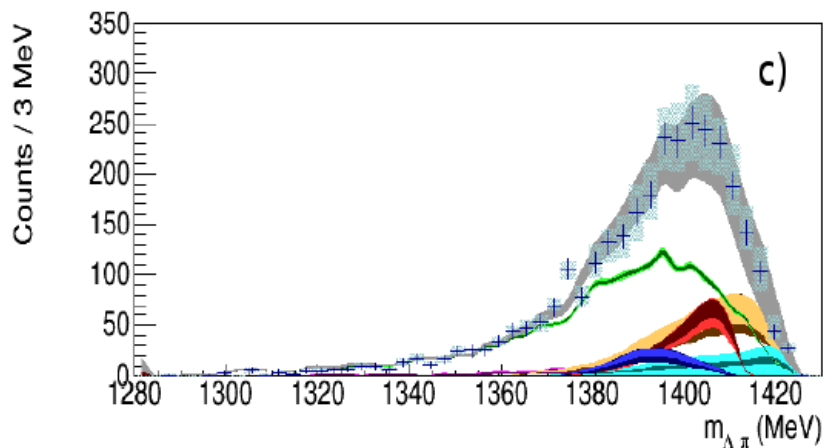
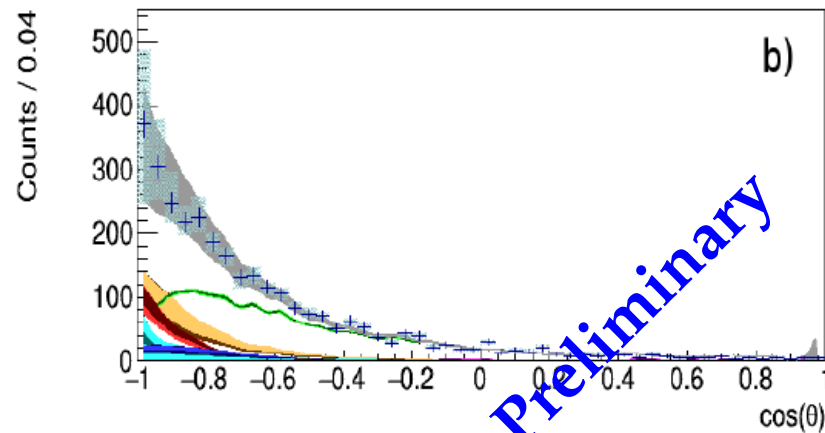
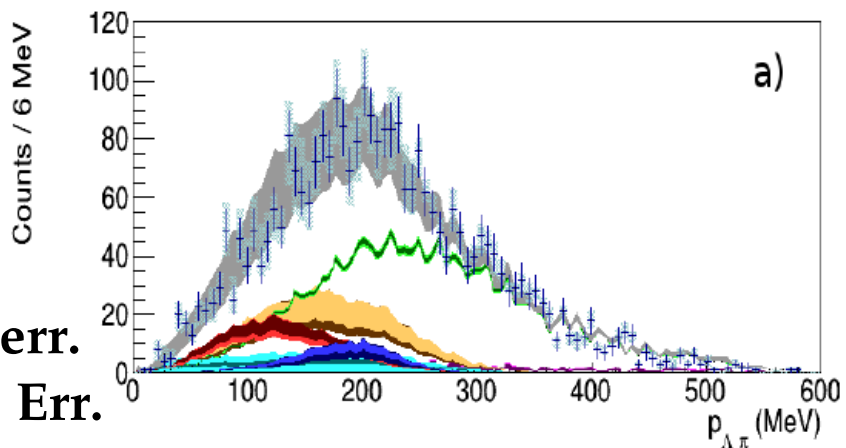


# Simultaneous momentum – angle – mass fit

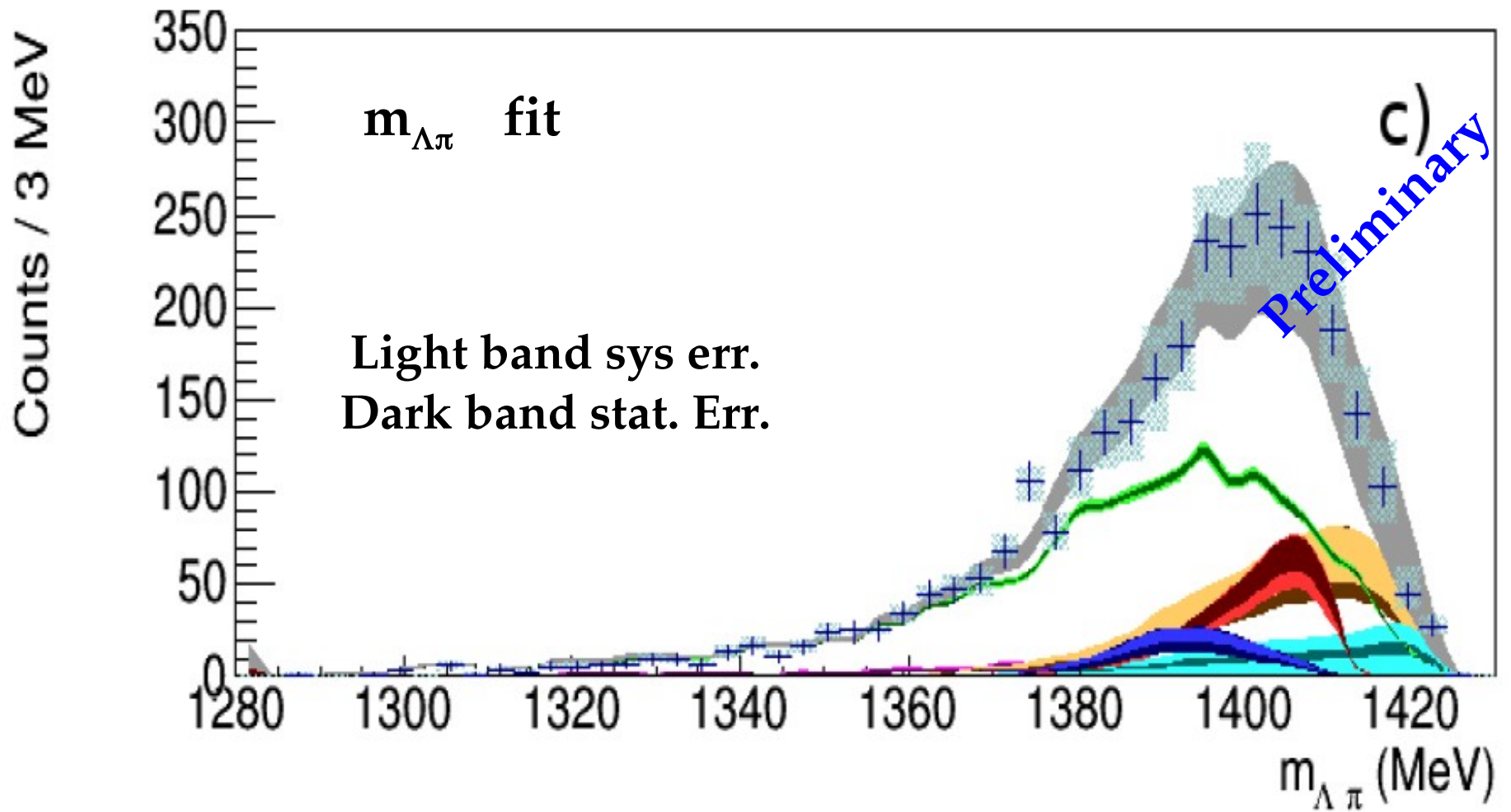
Light band sys err.  
Dark band stat. Err.

Non-Resonant  
(at-rest)  
(in-flight)

Resonant  $\Sigma^*$   
(at-rest)  
(in-flight)



# Comparison



**Non-Resonant**  
**(at-rest)**  
**(in-flight)**

**Resonant  $\Sigma^*$**   
**(at-rest)**  
**(in-flight)**

# Outcome of the measurement

From the well known  $\Sigma^*$  transition probability:

Preliminary

$$\frac{\text{NR} - \text{ar}}{\text{RES} - \text{ar}} = \frac{\int_0^{p_{max}} P_{ar}^{nr}(p_{\Lambda\pi}) dp_{\Lambda\pi}}{\int_0^{p_{max}} P_{ar}^{res}(p_{\Lambda\pi}) dp_{\Lambda\pi}} =$$

$$\Rightarrow |f_{ar}^s| = (0.334 \pm 0.018 \text{ stat}_{-0.058}^{+0.034} \text{ syst}) \text{ fm.}$$

$$= |f_{ar}^s|^2 \cdot 8,94 \cdot 10^5 \text{ MeV}^2 .$$

The sub-threshold result is compatible with corresponding values extracted from  $K^- p \rightarrow \Lambda \pi^0$  cross sections above threshold

J. K. Kim, Columbia University Report, Nevis 149 (1966)

J. K. Kim, Phys Rev Lett, 19 (1977) 1074:

$E = -33 \text{ MeV}$	$p_{lab} = 120 \text{ MeV}$	160 MeV	200 MeV	245 MeV
$0.334 \pm 0.018 \text{ stat}_{-0.058}^{+0.034} \text{ syst}$	0.33(11)	0.29(10)	0.24 (6)	0.28(2)

# Outcome of the measurement

$$|f_{ar}^s| = (0.334 \pm 0.018 \text{ stat}_{-0.058}^{+0.034} \text{ syst}) \text{ fm}.$$

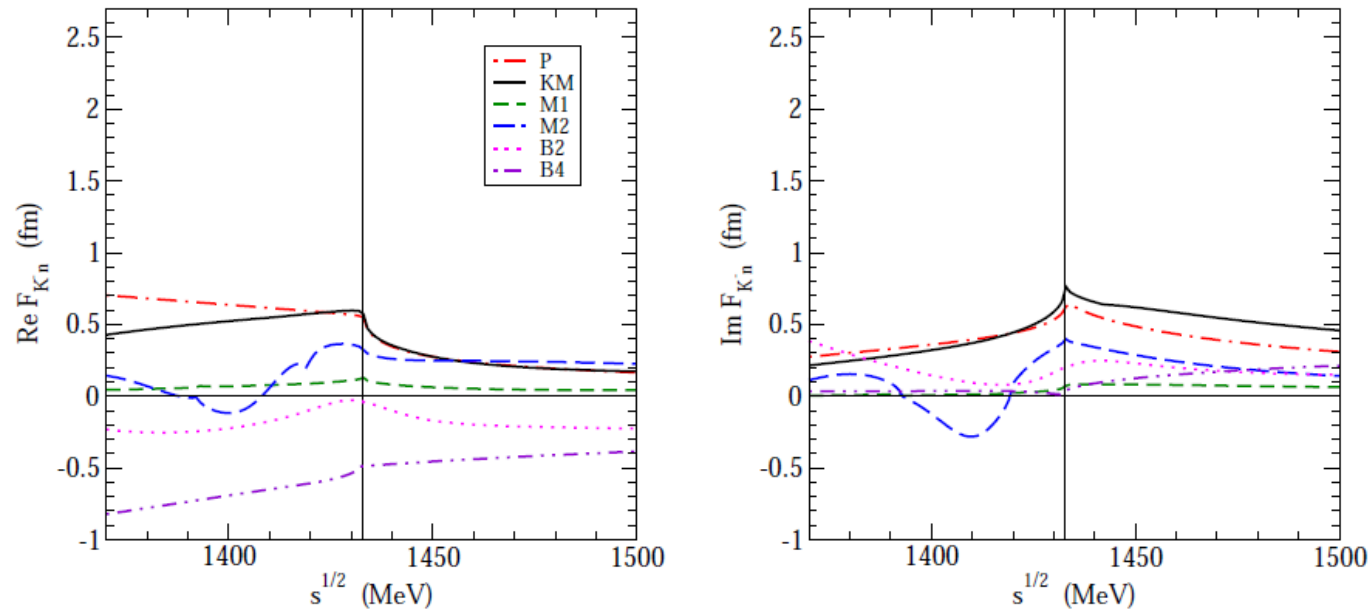


FIG. 1: Energy dependence of real (left) and imaginary (right) parts of free-space  $K^-p$  (top) and  $K^-n$  (bottom) amplitudes in considered chiral models (see text for details). Thin vertical lines mark threshold energies.

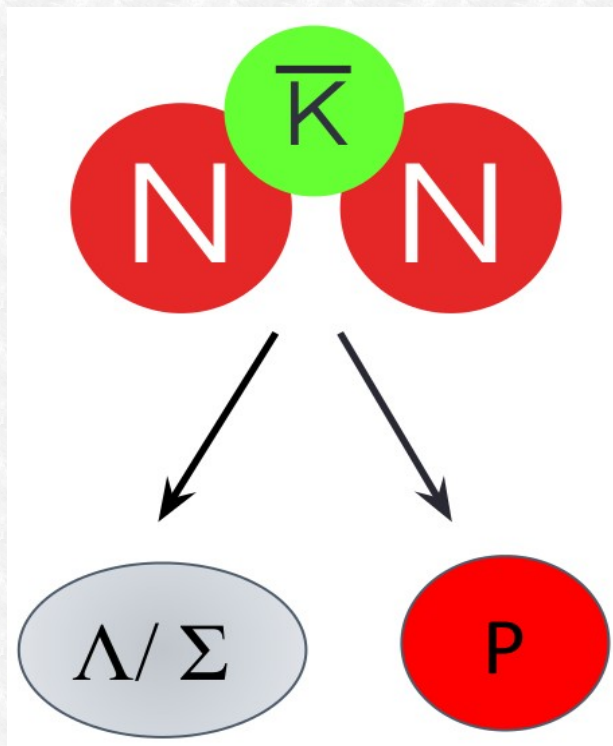
Preliminary

ArXiv:1704.07205v1 [nucl-th], accepted in Phys. Rev C  
Y. Ikeda, T. Hyodo and W. Weise, Nucl. Phys. A 881 (2012) 98.

**K<sup>-</sup> - multiN absorption and search  
for bound states**



# How deep can an antikaon be bound in a nucleus?



## Possible Bound States:

$$\begin{aligned} (K^- pp) &\rightarrow \Lambda p \\ &\rightarrow \Sigma^0 p \end{aligned}$$

$$\begin{aligned} (K^- ppn) &\rightarrow \Lambda d \\ &\rightarrow \Sigma^0 d \end{aligned}$$

predicted due to the strong  $\bar{K}N$  interaction in the  $I=0$  channel.

[Wycech (1986) - Akaishi & Yamazaki (2002)]

**K<sup>-</sup>pp bound state**

....at the end of 2015

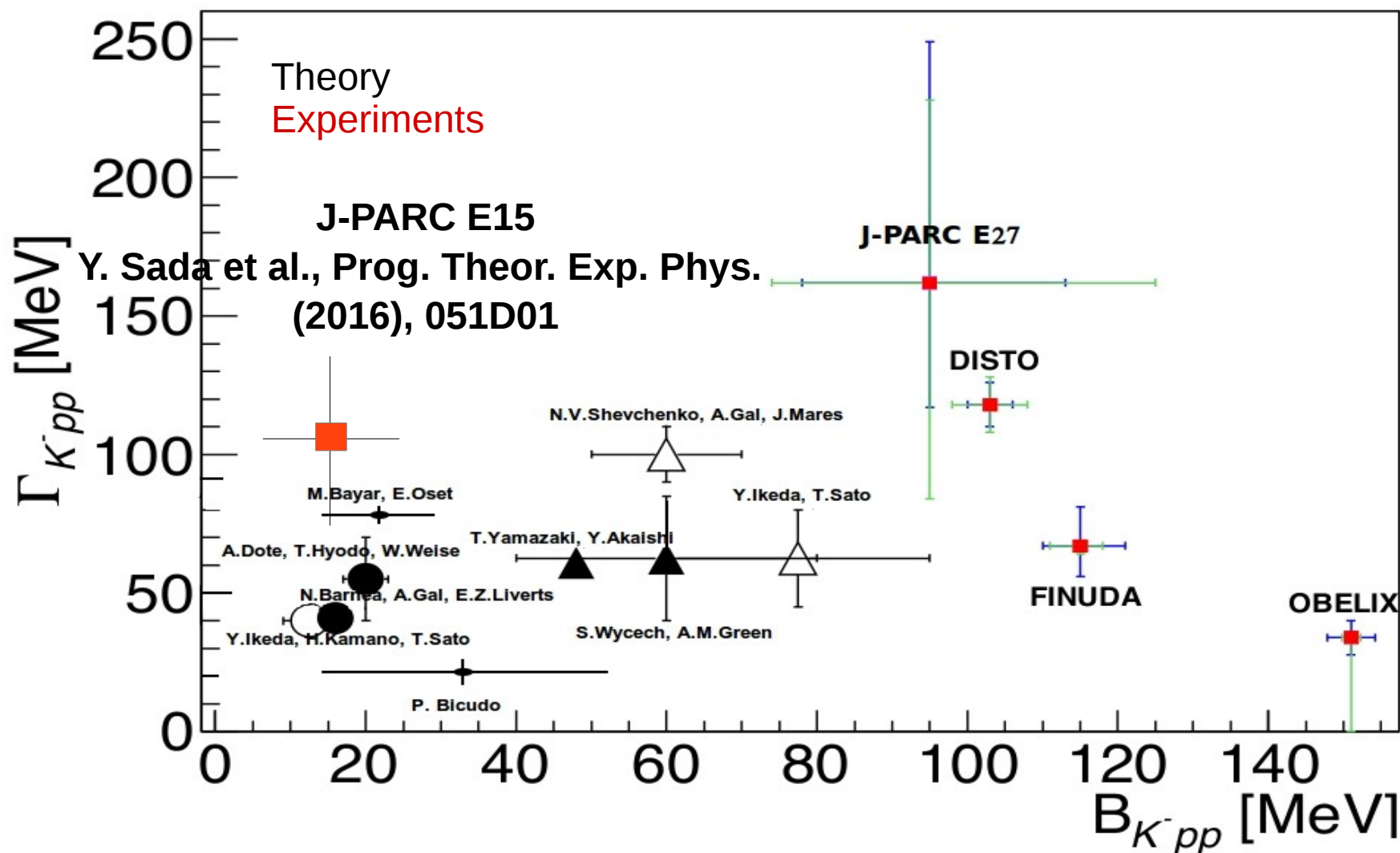
	BE (MeV)	$\Gamma$ (MeV)	Reference
Dote, Hyodo, Weise	17-23	40-70	Phys.Rev.C79 (2009) 014003
Akaishi, Yamazaki	48	61	Phys.Rev.C65 (2002) 044005
Barnea, Gal, Liverts	16	41	Phys.Lett.B712 (2012) 132-137
Ikeda, Sato	60-95	45-80	Phys.Rev.C76 (2007) 035203
Ikeda, Kamano, Sato	9-16	34-46	Prog.Theor.Phys. (2010) 124(3): 533
Shevchenko, Gal, Mares	55-70	90-110	Phys.Rev.Lett.98 (2007) 082301
Revai, Shevchenko	32	49	Phys.Rev.C90 (2014) no.3, 034004
Maeda, Akaishi, Yamazaki	51.5	61	Proc.Jpn.Acad.B 89, (2013) 418
Bicudo	14.2-53	13.8-28.3	Phys.Rev.D76 (2007) 031502
Bayar, Oset	15-30	75-80	Nucl.Phys.A914 (2013) 349
Wycech, Green	40-80	40-85	Phys.Rev.C79 (2009) 014001

Experiments reporting DBKNS		
<b>KEK-PS E549</b>	T. Suzuki et al. MPLA23, 2520-2523 (2008)	
<b>FINUDA</b>	M. Agnello et al. PRL94, 212303 (2005)	Extraction of a <b>signal</b>
<b>DISTO</b>	T. Yamazaki et al. PRL104 (2010)	Extraction of a <b>signal</b>
<b>OBELIX</b>	G. Bendiscioli et al. NPA789, 222 (2007)	Extraction of a <b>signal</b>
<b>HADES</b>	G. Agakishiev et al. PLB742, 242-248 (2015)	<b>Upper limit</b>
<b>LEPS/SPring-8</b>	A.O. Tokiyasu et al. PLB728, 616-621 (2014)	<b>Upper limit</b>
<b>J-PARC E15</b>	T. Hashimoto et al. PTEP, 061D01 (2015)	<b>Upper limit</b>
<b>J-PARC E27</b>	Y. Ichikawa et al. PTEP, 021D01 (2015)	Extraction of a <b>signal</b>

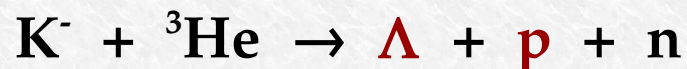
# How deep can an antikaon be bound in a nucleus?

interpreted in

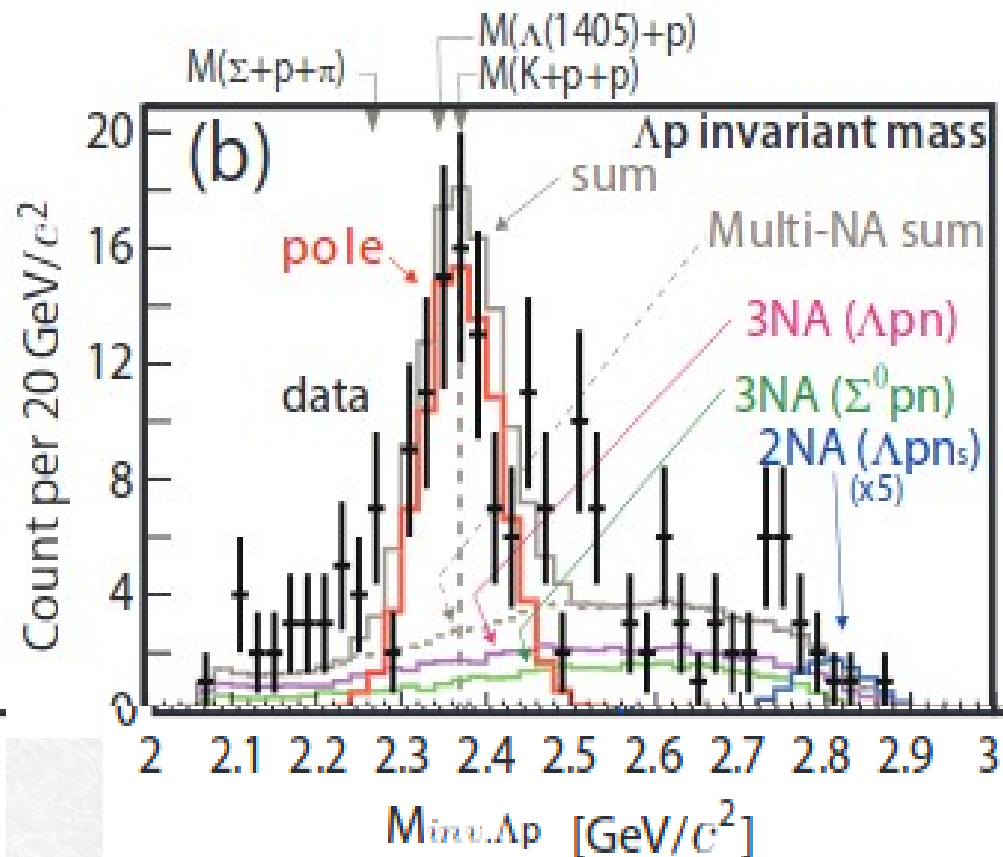
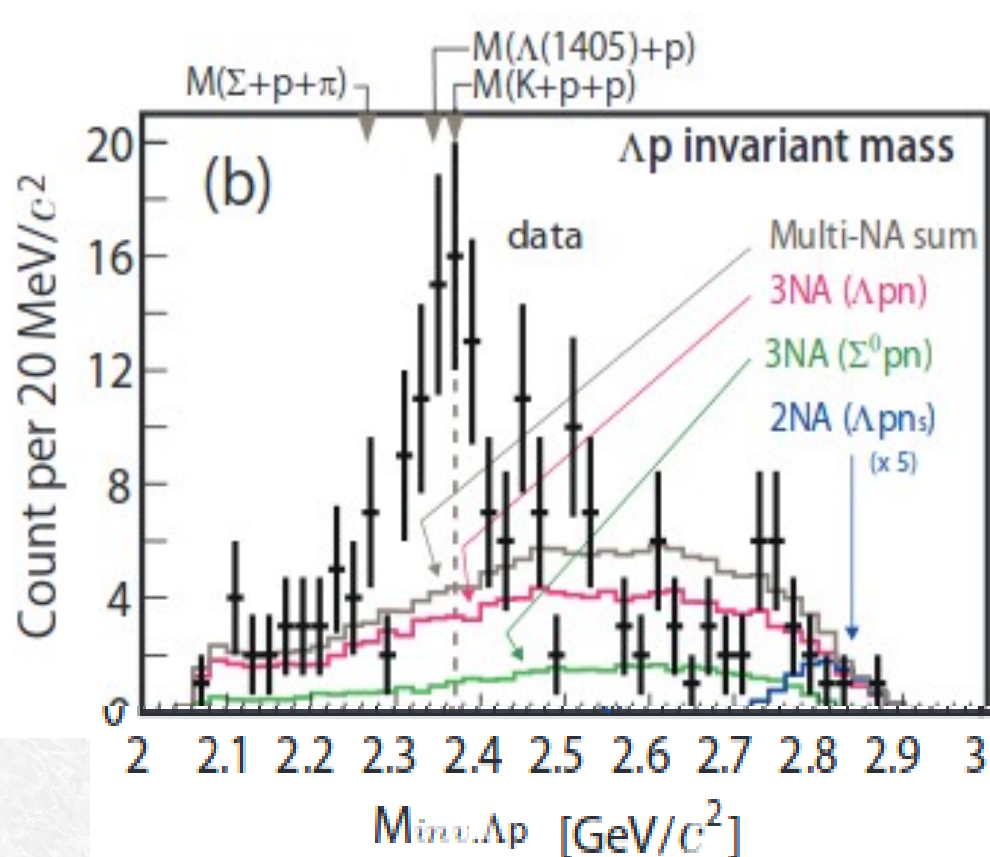
T. Sekihara, E. Oset, A. Ramos, Prog. Theor. Exp. Phys (2016) (12): 123D03



# J-PARC E15



Invariant mass spectroscopy



[J-PARC E15 Collaboration: arXiv:1601.06876 [nucl-ex]]

$M = 2355 +6 -8 \text{ (stat.)} \pm 12 \text{ (syst.) MeV}/c^2$   
 $\Gamma = 110 +19 -17 \text{ (stat.)} \pm 27 \text{ (syst.) MeV}/c^2$

BE = 15 MeV



**4NA cross section and yield**

## $\Lambda t$ available data

Available data:

- in Helium :

- bubble chamber experiment

[M.Roosen, J.H. Wickens, Il Nuovo Cimento 66, (1981), 101]

$K^-$  stopped in liquid helium,  $\Lambda$  dn/t search. **3 events** compatible with the  $\Lambda t$  kinematics were found

$$\text{BR}(K^-4\text{He} \rightarrow \Lambda t) = (3 \pm 2) \times 10^{-4} / K_{\text{stop}} \quad \text{global, no 4NA}$$

- Solid targets

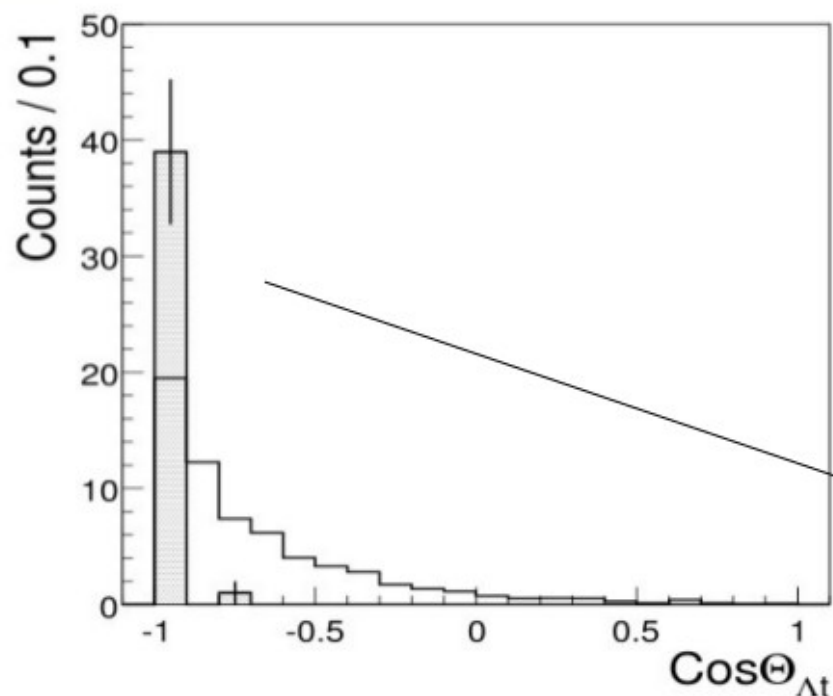
- FINUDA [Phys.Lett. B669 (2008) 229]

(**40 events** in different solid targets)

## $\Lambda t$ available data

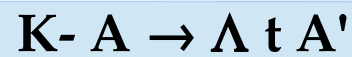
FINUDA presented [Phys.Lett.B (2008) 229]:

- a study of  $\Lambda$  vs  $t$  momentum correlation and an opening angle distribution
- **40 events** collected and added together coming from different targets ( ${}^6,7\text{Li}$ ,  ${}^9\text{Be}$ )



Filled histogram= data

Open histogram = Phase space simulation



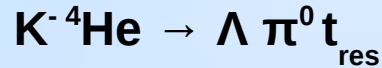
Unclear back to back topology

$\Lambda t$  emission yield  $\rightarrow 10^{-3} - 10^{-4} / K^-_{\text{stop}}$   
global, no 4NA

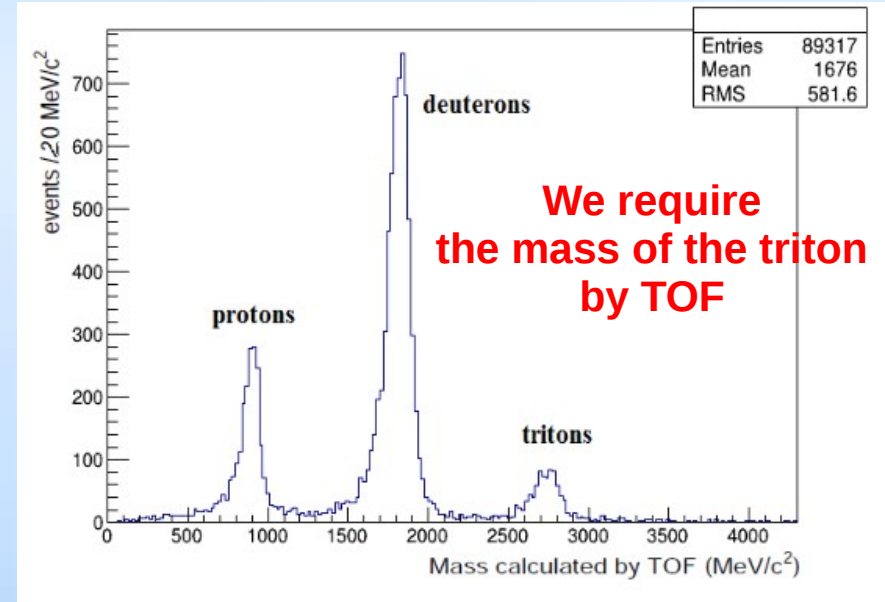
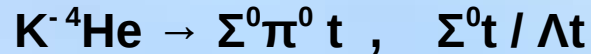
Experimental data only back-to-back

# $\Lambda t$ correlation studies in $^4\text{He}$ from the DC gas : contributing processes

single nucleon absorption (1NA)



conversion on triton:



Tritons are spectators, **too low momentum:**  $p_t \sim$  Fermi momentum

lower then the calorimeter threshold ( $p_t \sim 500 \text{ MeV}/c$ )

checked by MC simulations

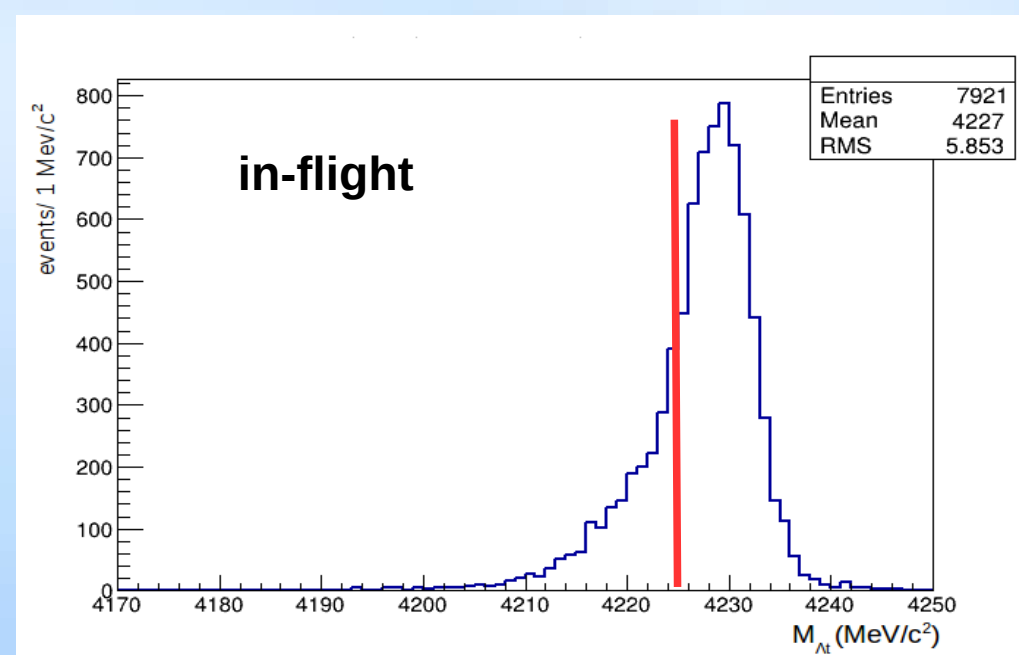
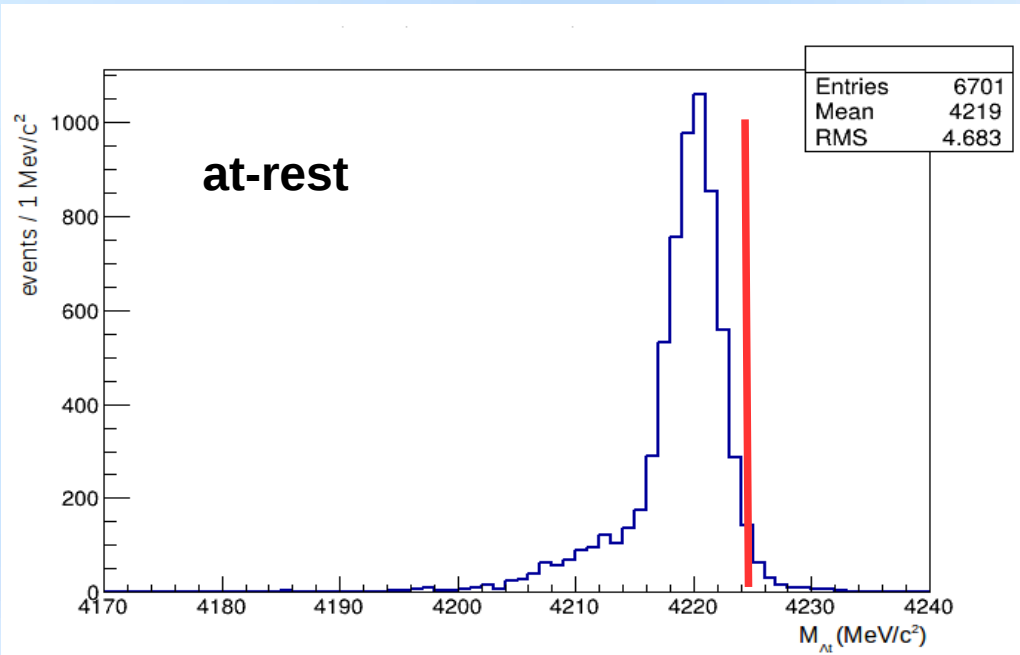
**4NA processes –  $K^-$  absorbed by the  $\alpha$  particle:**



conversion is suppressed  
by the  
 $\Sigma^0 - t$

**Back to back topology!**

# MC simulations: efficiency & resolution



mass threshold at-rest

M<sub>Λt</sub> invariant mass resolution = 2.2 MeV/c<sup>2</sup>

overall detection + reconstruction efficiency for 4NA direct Λt production :

$$\epsilon_{4\text{NA},ar,\Lambda t} = 0.0493 \pm 0.0006 \quad ; \quad \epsilon_{4\text{NA},if,\Lambda t} = 0.0578 \pm 0.0006,$$

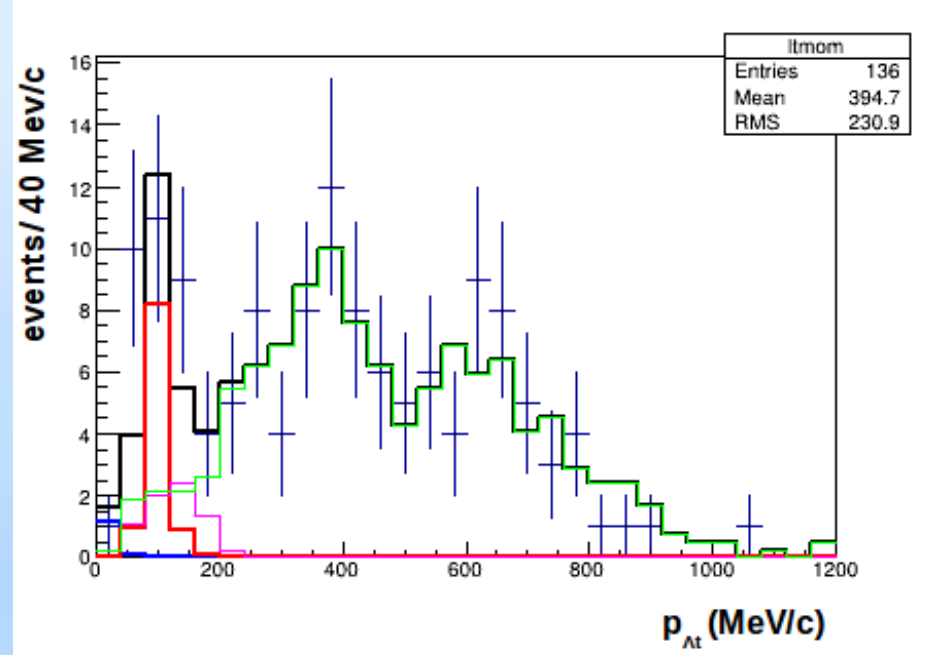
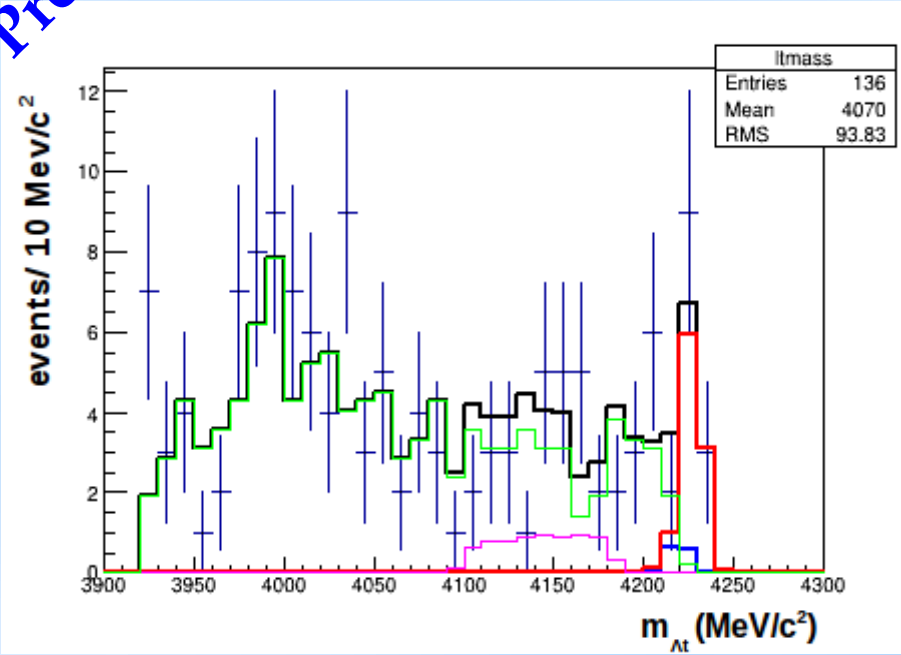
at-rest

in-flight



Preliminary

# $K^- ^4\text{He} \rightarrow \Lambda t$ 4NA cross section



+ data

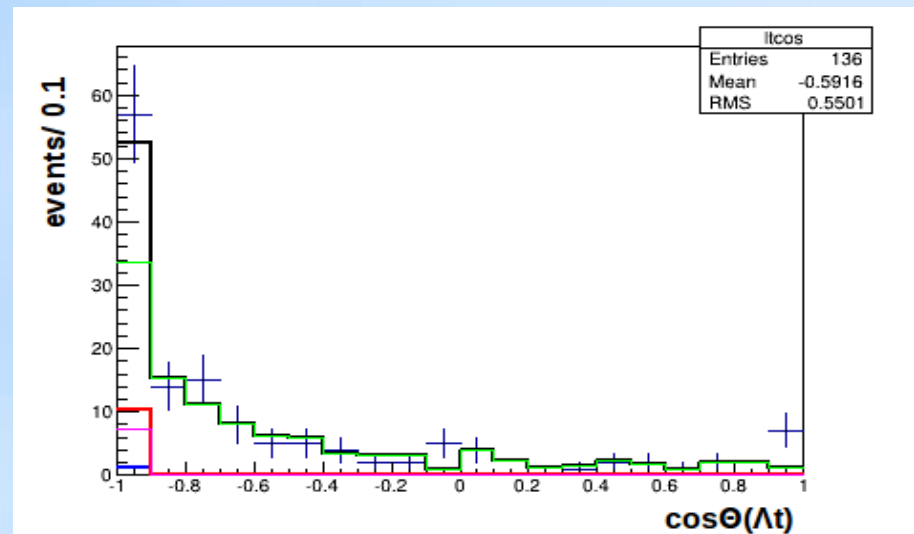
--- carbon data from DC wall

--- 4NA  $K^- ^4\text{He} \rightarrow \Lambda t$  in flight MC

--- 4NA  $K^- ^4\text{He} \rightarrow \Lambda t$  at rest MC

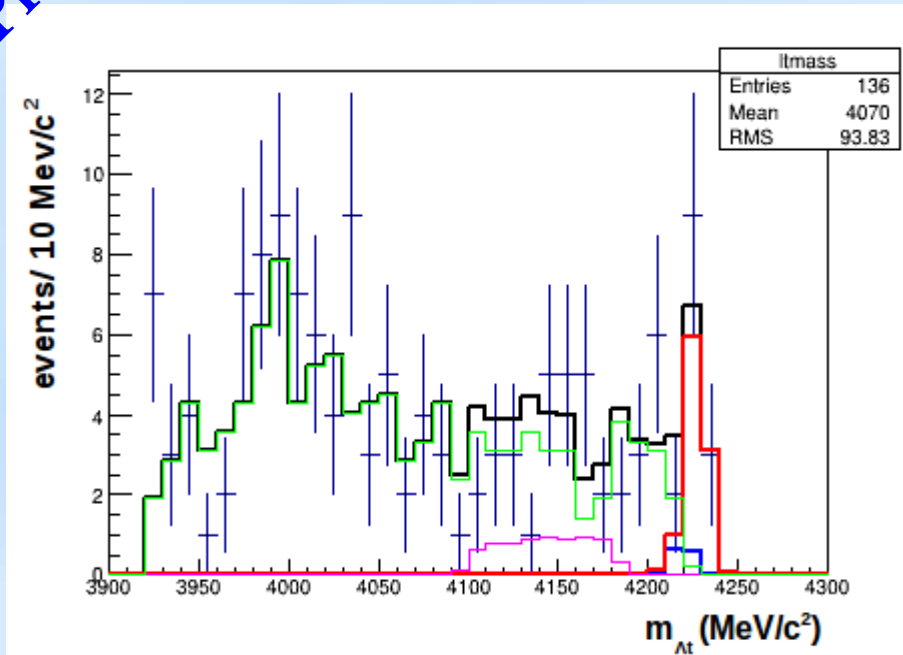
--- 4NA  $K^- ^4\text{He} \rightarrow \Sigma^0 t$ ,  $\Sigma^0 \rightarrow \Lambda \gamma$  MC

--- 4NA  $K^- ^4\text{He} \rightarrow \Sigma^0 t$ ,  $\Sigma^0 \rightarrow \Lambda \gamma$  MC



Preliminary

# K-<sup>4</sup>He → Λt 4NA cross section



Contribution to the spectra	Parameter value
$K^{-4}\text{He} \rightarrow \Lambda t$ at rest	$0.01 \pm 0.01$
$K^{-4}\text{He} \rightarrow \Lambda t$ in-flight	$0.09 \pm 0.02$
$K^{-4}\text{He} \rightarrow \Sigma^0 t$ in-flight	$0.05 \pm 0.03$
$K^{-12}\text{C} \rightarrow \Lambda t$ experimental distribution from the carbon DC wall	$0.85 \pm 0.06$
$\chi^2 / \text{ndf}$	0.654

Total number of events = 136

4NA K<sup>-4</sup>He → Λt at rest → 1 ± 1 events

4NA K<sup>-4</sup>He → Λt in flight → 12 ± 3 events

+ data

--- carbon data from DC wall

--- 4NA K<sup>-4</sup>He → Λt in flight MC

--- 4NA K<sup>-4</sup>He → Λt at rest MC

--- 4NA K<sup>-4</sup>He → Σ<sup>0</sup>t , Σ<sup>0</sup> → Λγ MC

--- 4NA K<sup>-4</sup>He → Σ<sup>0</sup>t , Σ<sup>0</sup> → Λγ MC

$$\text{BR}(K^{-4}\text{He}(4\text{NA}) \rightarrow \Lambda t) < 1.3 \times 10^{-4} / K_{\text{stop}}$$

$$\begin{aligned} \sigma(100 \pm 19 \text{ MeV}/c) (K^{-4}\text{He}(4\text{NA}) \rightarrow \Lambda t) = \\ = (0.42 \pm 0.13(\text{stat})^{+0.01}_{-0.02} (\text{syst})) \text{ mb} \end{aligned}$$

## perspectives:

- **Sub-threshold  $K^- n \rightarrow \Lambda \pi^-$  non resonant amplitude**

Nucl. Phys. A954 (2016) 75-93

$$|f_{ar}^s| = (0.334 \pm 0.018_{\text{stat}}^{+0.034}_{-0.058} \text{syst}) \text{ fm}.$$

experimental paper finalised

next step extract the same info in  $l = 0$  to interpret the  $\Sigma^0 \pi^0$  spectra

- **K- multiN absorption yields in  $\Sigma^0 p$**  Physics Letters B 758 (2016) 134

	yield / $K_{stop}^- \cdot 10^{-2}$	$\sigma_{stat} \cdot 10^{-2}$	$\sigma_{syst} \cdot 10^{-2}$
2NA-QF	0.127	$\pm 0.019$	$+0.004$ $-0.008$

Same analysis is ongoing in  $\Lambda p$  (R. Del Grande PhD thesis)

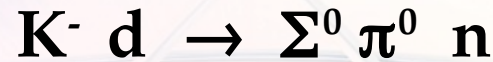
- **K-  $^4\text{He} \rightarrow \Lambda t$  4NA cross section**  $\sigma(100 \pm 19 \text{ MeV/c}) (K^- ^4\text{He}(4\text{NA}) \rightarrow \Lambda t) =$   
 $= (0.42 \pm 0.13(\text{stat})^{+0.01}_{-0.02} (\text{syst})) \text{ mb}$  paper in preparation

- **feasibility study of the  $\Sigma^0$  - N/NN two and three body forces**  
measurement from K-absorption in  $^4\text{He}$

# *AMADEUS physics case*

$K^-$

- establish the nature of the  $\Lambda(1405)$  through the reaction:



- search for K-multiN clusters, possible reactions:

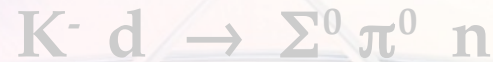


- $Y - N/NN$  two & three body interaction (ex.  $\Sigma^0 - N/NN$  from  $K^- {}^4\text{He}$  induced reactions)
- $K^\pm N$  elastic & inelastic scattering below 100 MeV
  - also low momentum  $K^\pm {}_Z^AX$  scattering for low Z gas targets
- Neutron rich hypernuclei

# *AMADEUS physics case*

$K^-$

- establish the nature of the  $\Lambda(1405)$  through the reaction:



- search for K-multiN clusters, possible reactions:



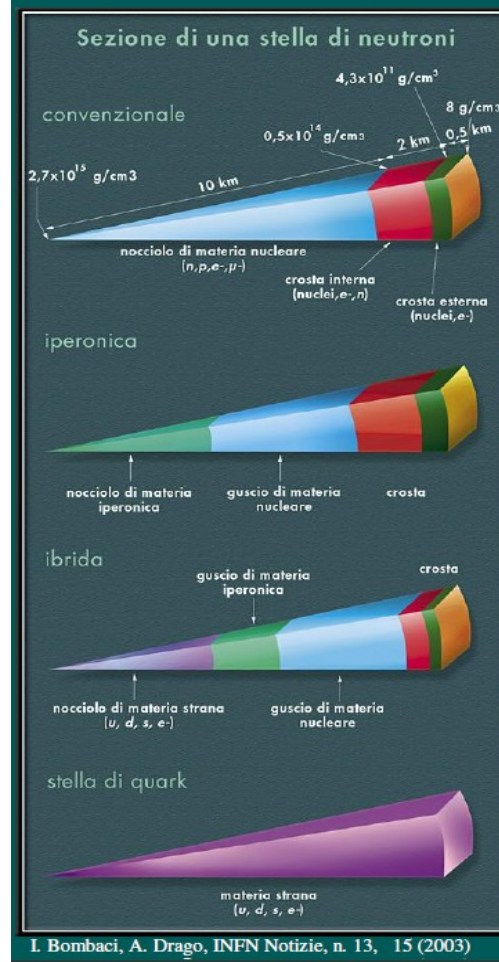
- **$\Upsilon - N/NN$  two & three body interaction (ex.  $\Sigma^0 - N/NN$  from  $K^- {}^4\text{He}$  induced reactions)**

- $K^\pm N$  elastic & inelastic scattering below 100 MeV

- also low momentum  $K^\pm {}_Z^AX$  scattering for low Z gas targets

- Neutron rich hypernuclei

# Y-N/NN interaction essential impact on the case of NEUTRON STARS



“Neutron  
Nucleon Stars  
Hyperon Stars  
Hybrid Stars  
Strange Stars

## Microscopic approach to hyperonic matter EOS

input

**2BF: nucleon-nucleon (NN), nucleon-hyperon (NY), hyperon-hyperon (YY)**  
e.g. Nijmegen, Julich models

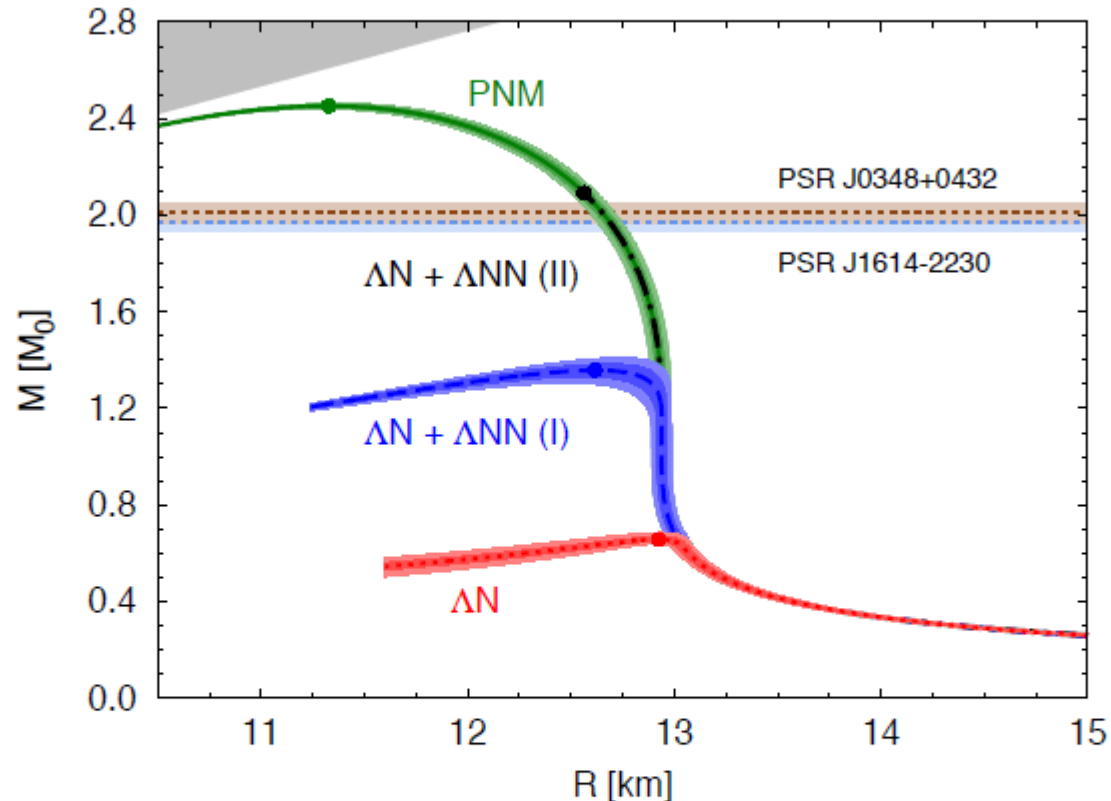
**3BF: NNN, NNY, NYY, YYY**

**Hyperonic sector: experimental data**

- YN scattering** (very few data)
- Hypernuclei**

# No experimental information on $\Sigma^0$ -N/NN interaction

## $\Lambda$ -neutron matter

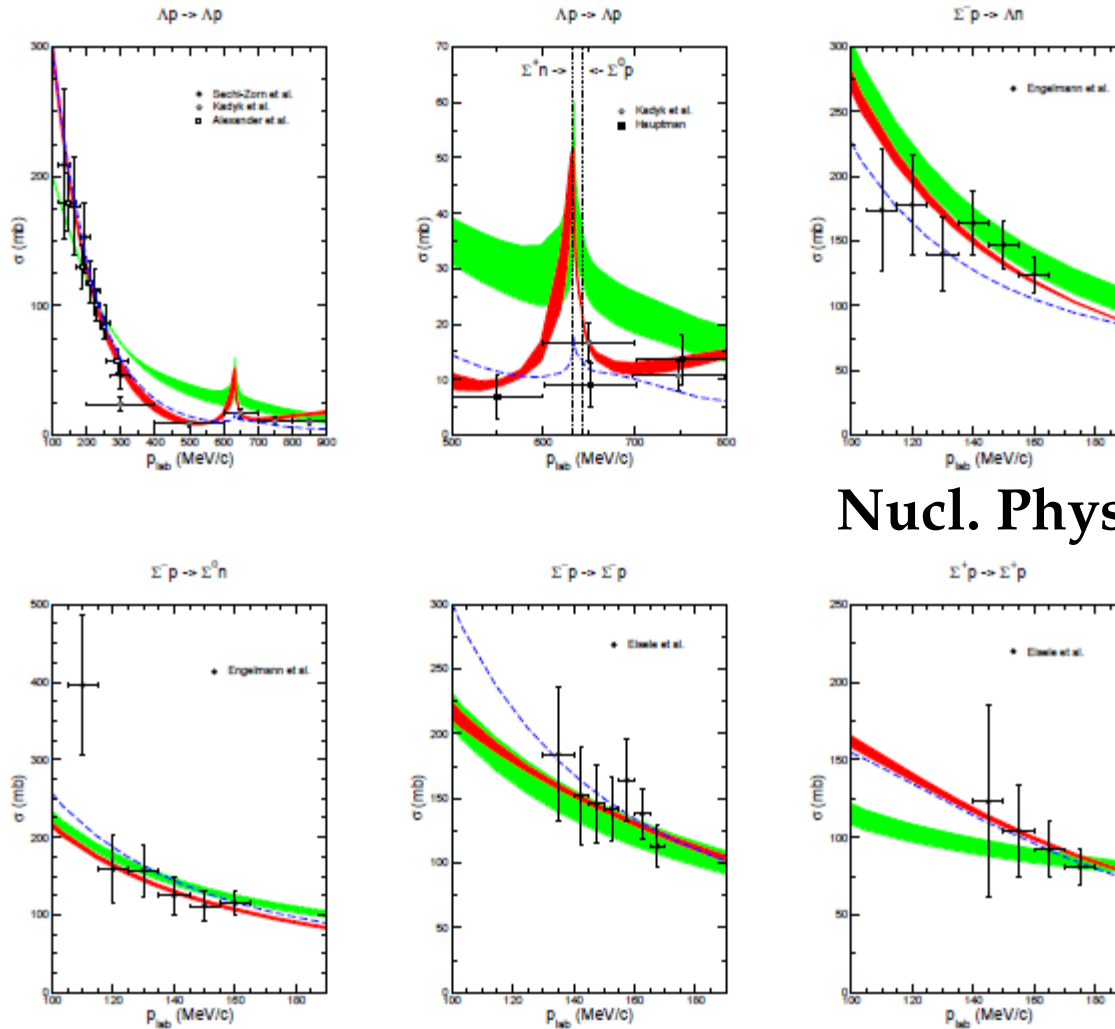


Lonardoni, Lovato, Gandolfi, Pederiva, PRL (2015)

Drastic role played by  $\Lambda NN$ . Calculations can be compatible with neutron star observations.

Note: no  $\nu_{\Lambda}$ , no protons, and no other hyperons included yet...

# No experimental information on $\Sigma^0$ -N/NN interaction



Nucl. Phys. A 915 (2013) 24-58

Figure 2: "Total" cross section  $\sigma$  (as defined in Eq. (24)) as a function of  $p_{\text{lab}}$ . The experimental cross sections are taken from Refs. [52] (filled circles), [53] (open squares), [65] (open circles), and [66] (filled squares) ( $\Lambda p \rightarrow \Lambda p$ ), from [54] ( $\Sigma^- p \rightarrow \Lambda n$ ,  $\Sigma^- p \rightarrow \Sigma^0 n$ ) and from [55] ( $\Sigma^- p \rightarrow \Sigma^- p$ ,  $\Sigma^+ p \rightarrow \Sigma^+ p$ ). The red/dark band shows the chiral EFT results to NLO for variations of the cutoff in the range  $\Lambda = 500, \dots, 650$  MeV, while the green/light band are results to LO for  $\Lambda = 550, \dots, 700$  MeV. The dashed curve is the result of the Jülich '04 meson-exchange potential [36].





$K^-$

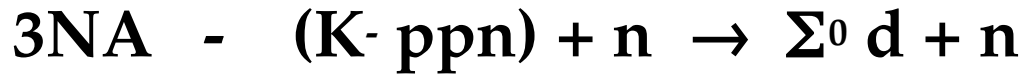


**3NA in  $^4\text{He}$**

**for the investigation of the**

**$\Sigma^0\text{-N}$  &  $\Sigma^0\text{-(NN)}$  interaction**

# Involved reactions:



- The  $\Sigma^0$  identification (with respect to  $\Lambda$ ) enables to **avoid the dominant internal conversion background**. Moreover there is presently no available  $\Sigma^0$ -N interaction data.

-  $^4\text{He}$  good target no **nuclear fragmentation can follow the 3NA** primary process.

3NA

1) W.O. F.S.I.

2) WITH  $\Sigma^0 d$  F.S.I.

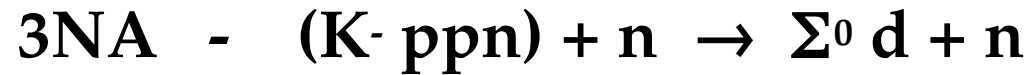
— IF F.S.I. IS MORE PROBABLE AMONG  $\Sigma^0 d$  (then  $\Sigma^0 n$  or  $d n$ ) THE RELATIVE YIELDS :

$$Y_{3NA,1} / Y_{3NA,2}$$

GIVE INFORMATION ON  $\Sigma^0 NN$  3body INTERACTION

— BACKGROUND:  $2NA (K^- pn) + d \rightarrow (\Lambda n) + d$

# Comparison with available data



Data correspond to K- captures in the  $^{12}\text{C}$  solid target.

We will show that the most energetic part of the  $m_{\Sigma^0 \text{d}}$  invariant mass spectrum, correlated with high  $p_{\Sigma^0}$  and  $p_{\text{d}}$  momenta, corresponds to the  $3\text{NA} - (\text{K- ppn})$  process

The  $\Sigma^0 \text{d}$  statistics corresponding to the sample of K- captures in the gas from the KLOE DC is much lower (1 order of mag.)

A dedicated measurement with pure  $^4\text{He}$  target is mandatory!!

## 3NA



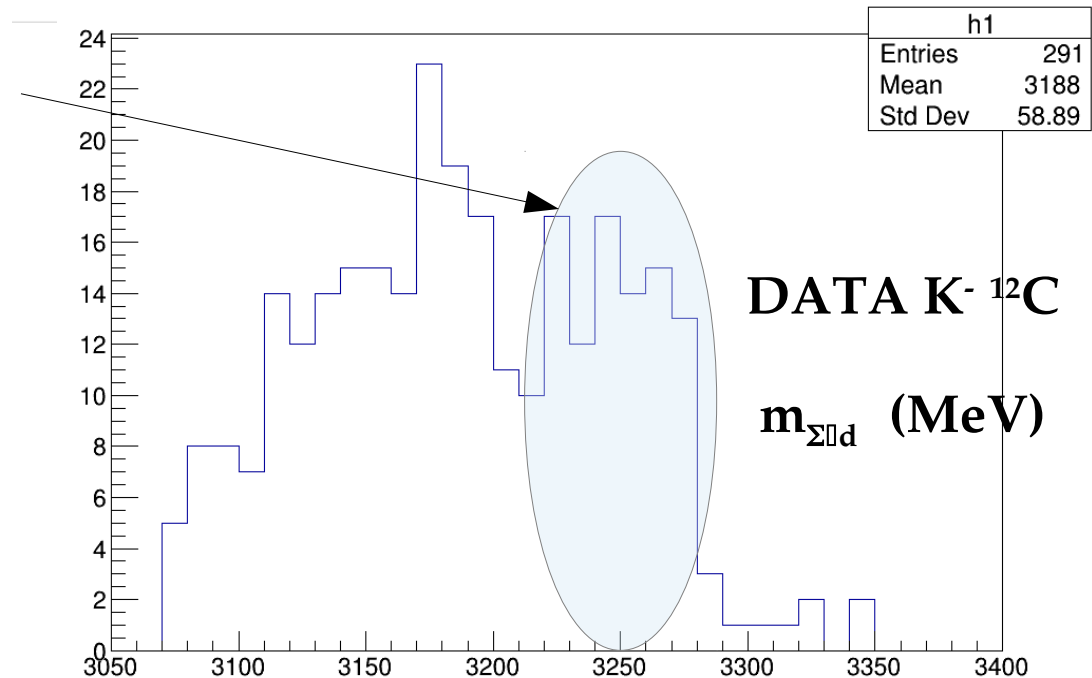
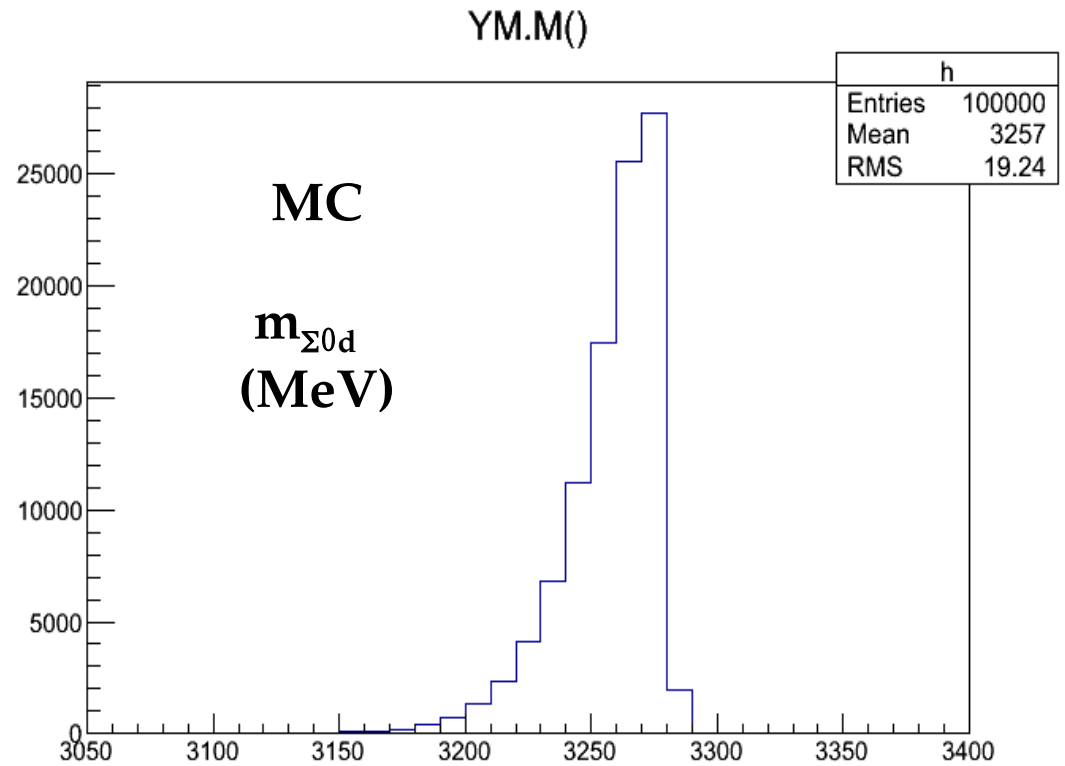
without FSI

Corresponds to the highest part of the invariant mass spectrum

the blue region is populated by:

free 3NA + 3NA followed FSI.

Lower energies (below 3220 MeV) probably involve 2NA and complex FSI processes with fragmentation of the residual  $^8\text{Be}$ .



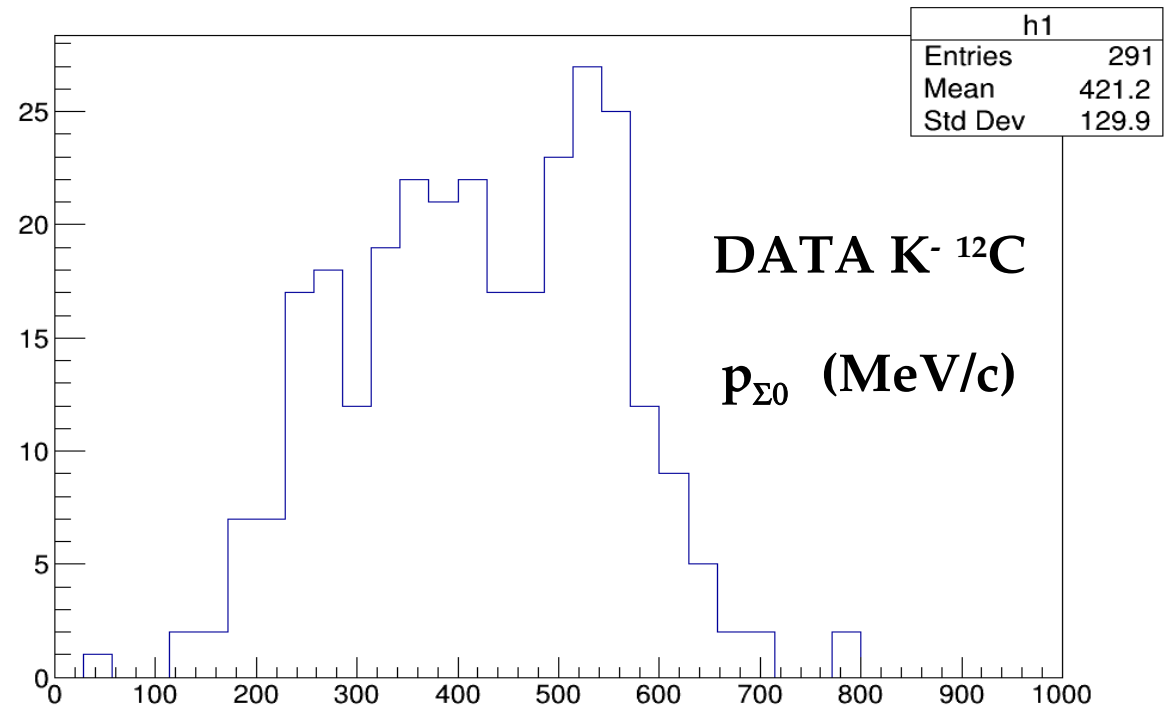
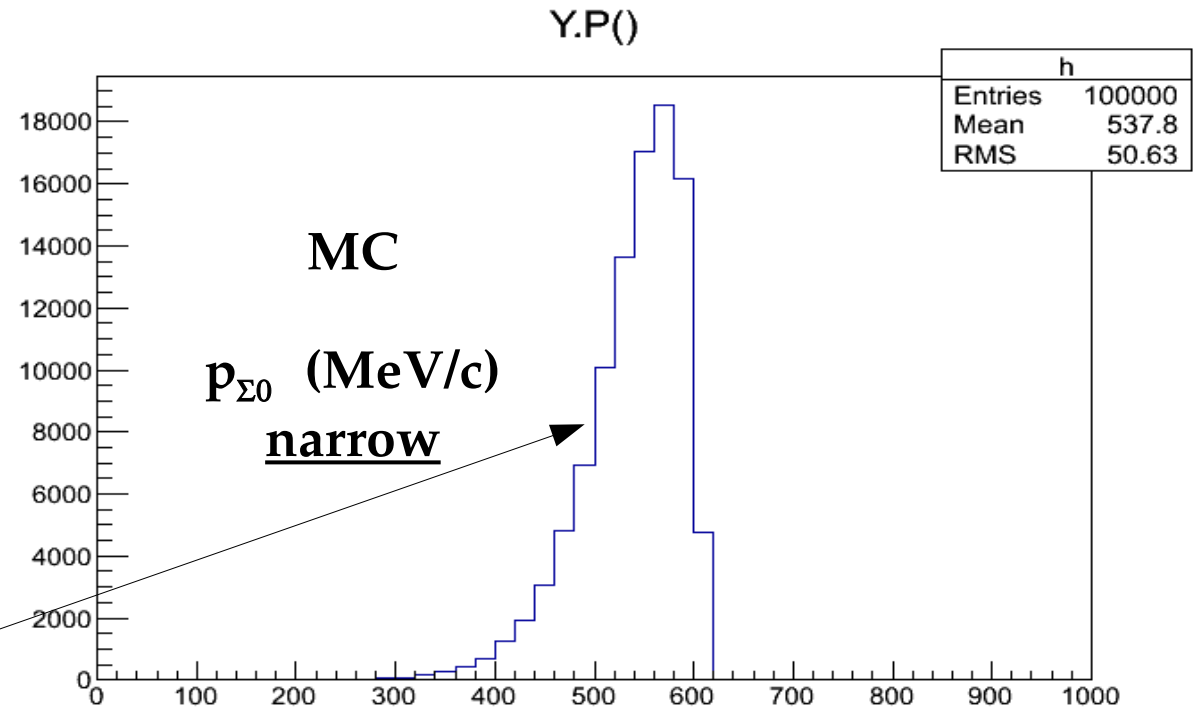
## 3NA



without FSI

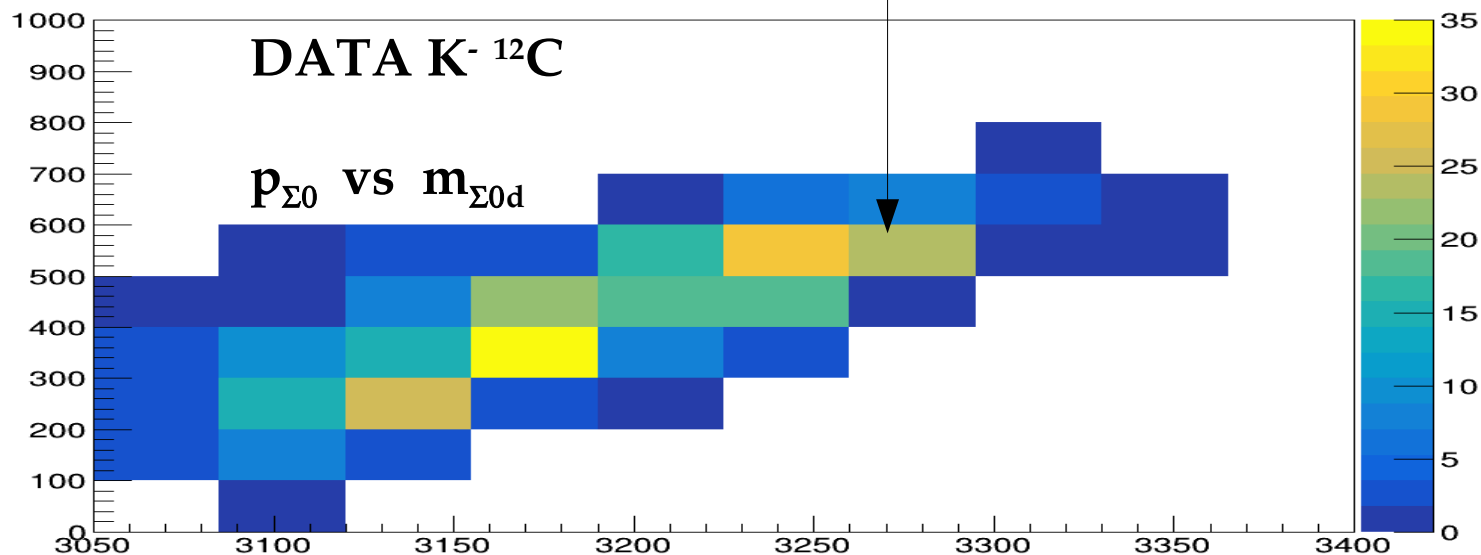
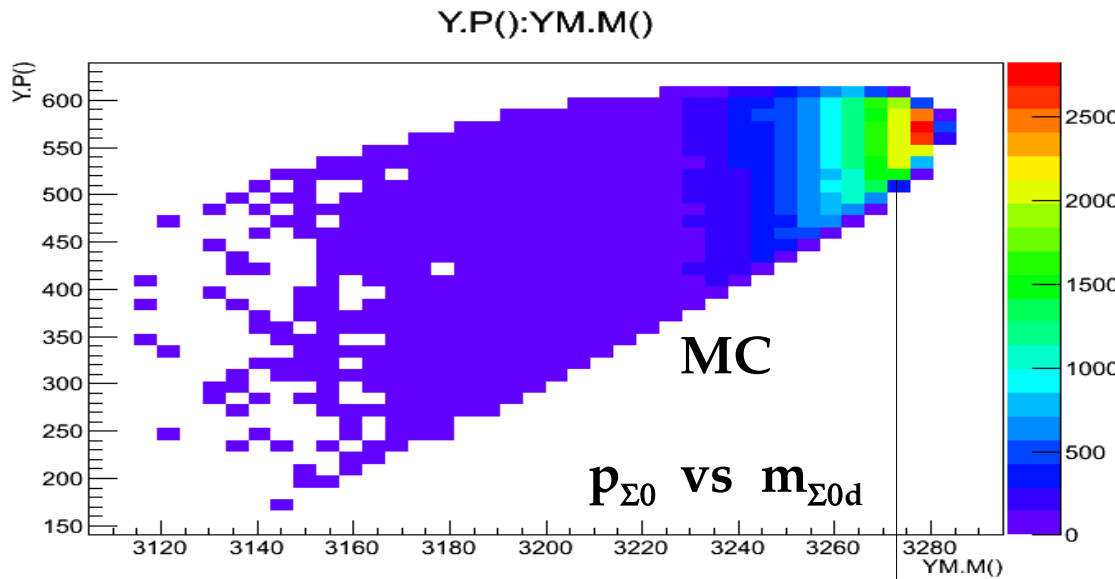
Corresponds to the highest part of the  $\Sigma^0$  momentum spectrum.

The narrow  $\Sigma^0$  momentum distribution will enable to  $\Sigma^0$ -NN cross section at  $550 \pm 50$  MeV/c.



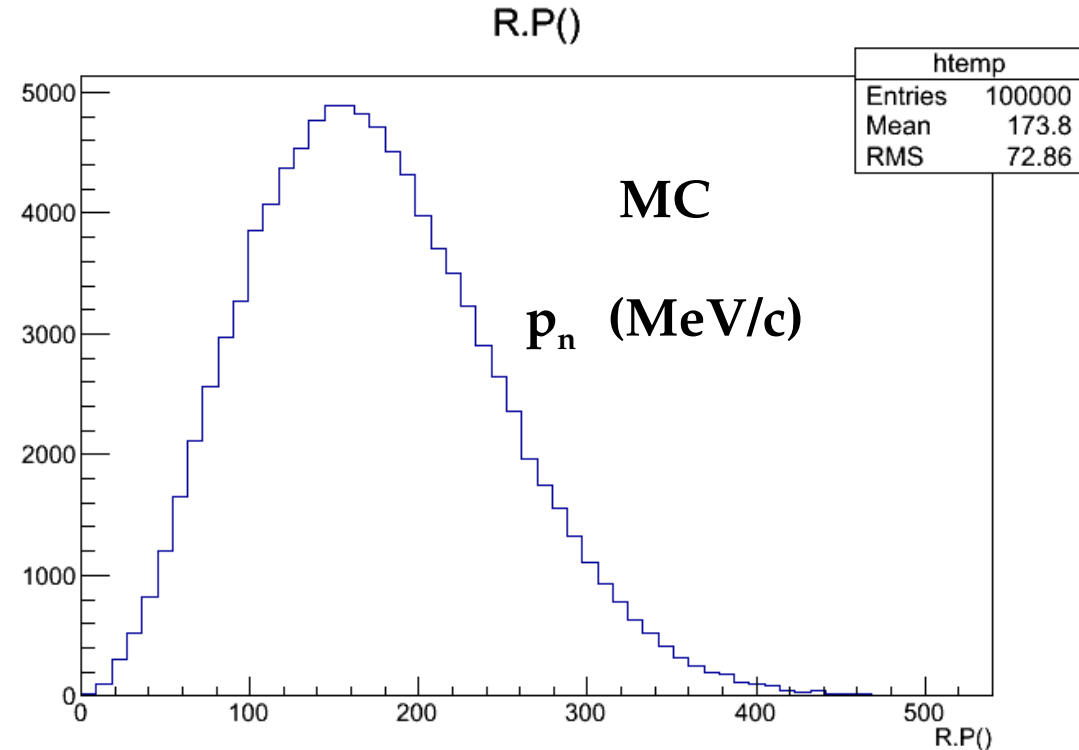
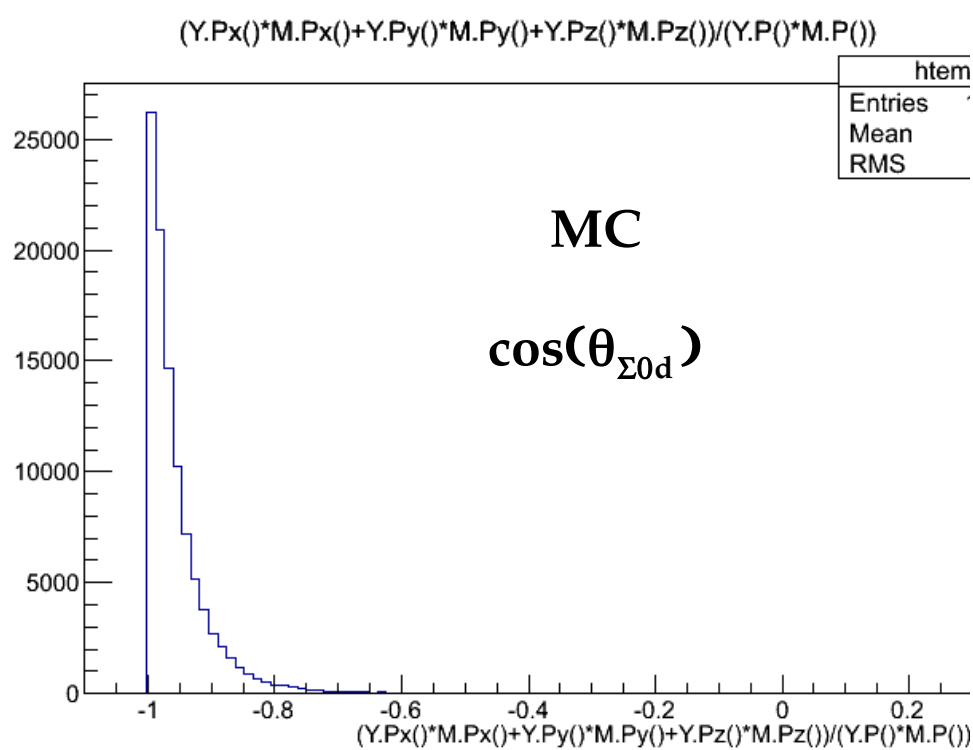
# 3NA (K-ppn) + n $\rightarrow$ $\Sigma^0$ d + n w. o. FSI

- clean mometum mass correlation



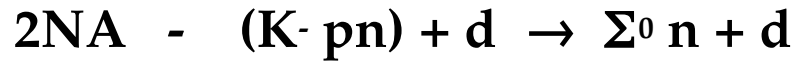
# 3NA - (K- ppn) + n $\rightarrow$ $\Sigma^0$ d + n signature:

- Highest  $\Sigma^0$  - d angular correlation
- low Fermi momentum neutron



# Using the same data set ...

The competing process



can be used to extract  
the complementary  
information:

$[2NA]$

1) W.O. F.S.I.

2) WITH F.S.I.

— IF F.S.I. IS MORE PROBABLE AMONG  $\Sigma^0$ -n (than  $\Sigma^0$ -d or n-d) THE RELATIVE YIELDS

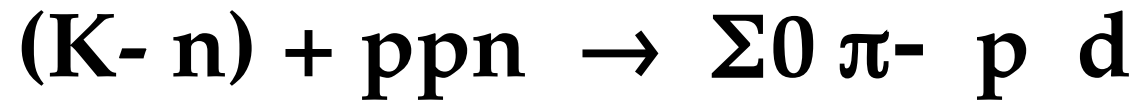
$$Y_{2NA,1} / Y_{2NA,2}$$

GIVE INFORMATION ON THE  $\Sigma^0$ n 2 body interaction

— CONSTRAINT: GLOBAL 2NA @ 3NA Yields MUST BE COMPATIBLE!



## Background reactions:



- low energy (took away by the pion) not correlated  $\Sigma^0$  d pairs.  
It is easy to be disentangled (similar to the  $\Sigma^0$  p analysis).

# **Accurate calculations of the FSI processes**

**are needed to extract the corresponding  
cross sections from the measured shapes.**

# *AMADEUS physics case*

$K^-$

- establish the nature of the  $\Lambda(1405)$  through the reaction:



- search for K-multiN clusters, possible reactions:



- $\Upsilon - N/NN$  two & three body interaction (ex.  $\Sigma^0 - N/NN$  from  $K^- {}^4\text{He}$  induced reactions)

- **$K^\pm N$  elastic & inelastic scattering below 100 MeV**

- also low momentum  $K^\pm {}_Z^AX$  scattering for low Z gas targets

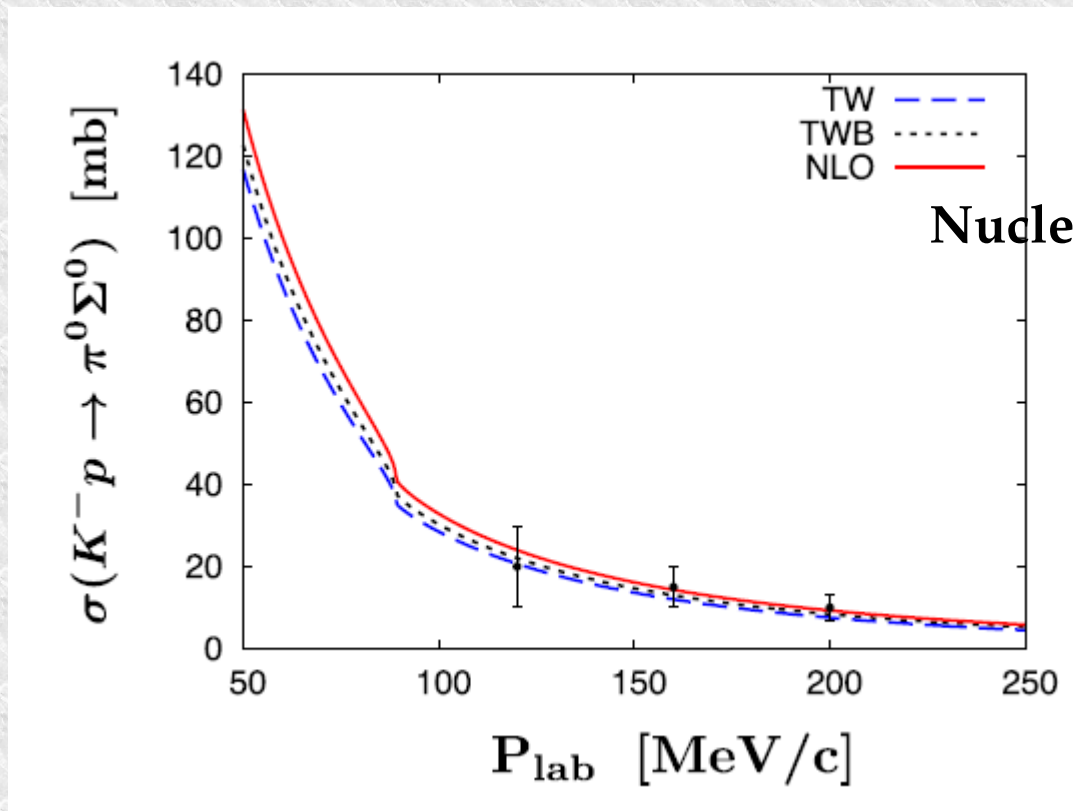
- Neutron rich hypernuclei

$K^- p \rightarrow \Sigma^0 \pi^0$  cross section measurement  
at  $p_K \sim 100 \text{ MeV}/c$



# $K^- N$ cross section measurement at $p_K = 100 \text{ MeV}/c$ , an example..

- $K^- p \rightarrow \Sigma^0 \pi^0$  cross section measurement at or below  $100 \text{ MeV}/c$  missing
- existing data at (120, 160, ..)  $\text{MeV}/c$  with big relative errors (about 50% & 120  $\text{MeV}/c$ )



Nuclear Physics A 881 (2012) 98–114

# $K^- p \rightarrow \Sigma^0 \pi^0$ cross section measurement the strategy

We employ the following reaction, where  $p=H$  is a “quasi-free” proton in the  $C_4H_{10}$  molecule

$$K^- p \rightarrow \Sigma^0 \pi^0 \rightarrow (\Lambda(1116) \gamma_3) (\gamma_1 \gamma_2) \rightarrow (p \pi^-) 3\gamma$$

- First we identify the  $\Lambda(1116)$  through its decay in pion and proton
  - then photon clusters are identified:

# Photons selection

1) Select events with at least three neutral clusters ( $E_{c1} > 20$  MeV) not from K decay ( $K^+ \rightarrow \pi^+ \pi^0$ )

2) **photon clusters selection:** a first minimization is performed  $\chi_t^2 = t^2/\sigma_t^2$  where  $t = t_i - t_j$  is the difference between time of flights in light speed hypothesis.

This selects three photon clusters in time from the  $\Lambda$  decay vertex  $\mathbf{r}_\Lambda$ .

3) **photon clusters identification:** to distinguish photon clusters from  $\pi^0$  decay, from  $\gamma_3$  (due to  $\Sigma^0$  decay) a second minimization is performed on  $\chi_{\pi\Sigma}^2$ :

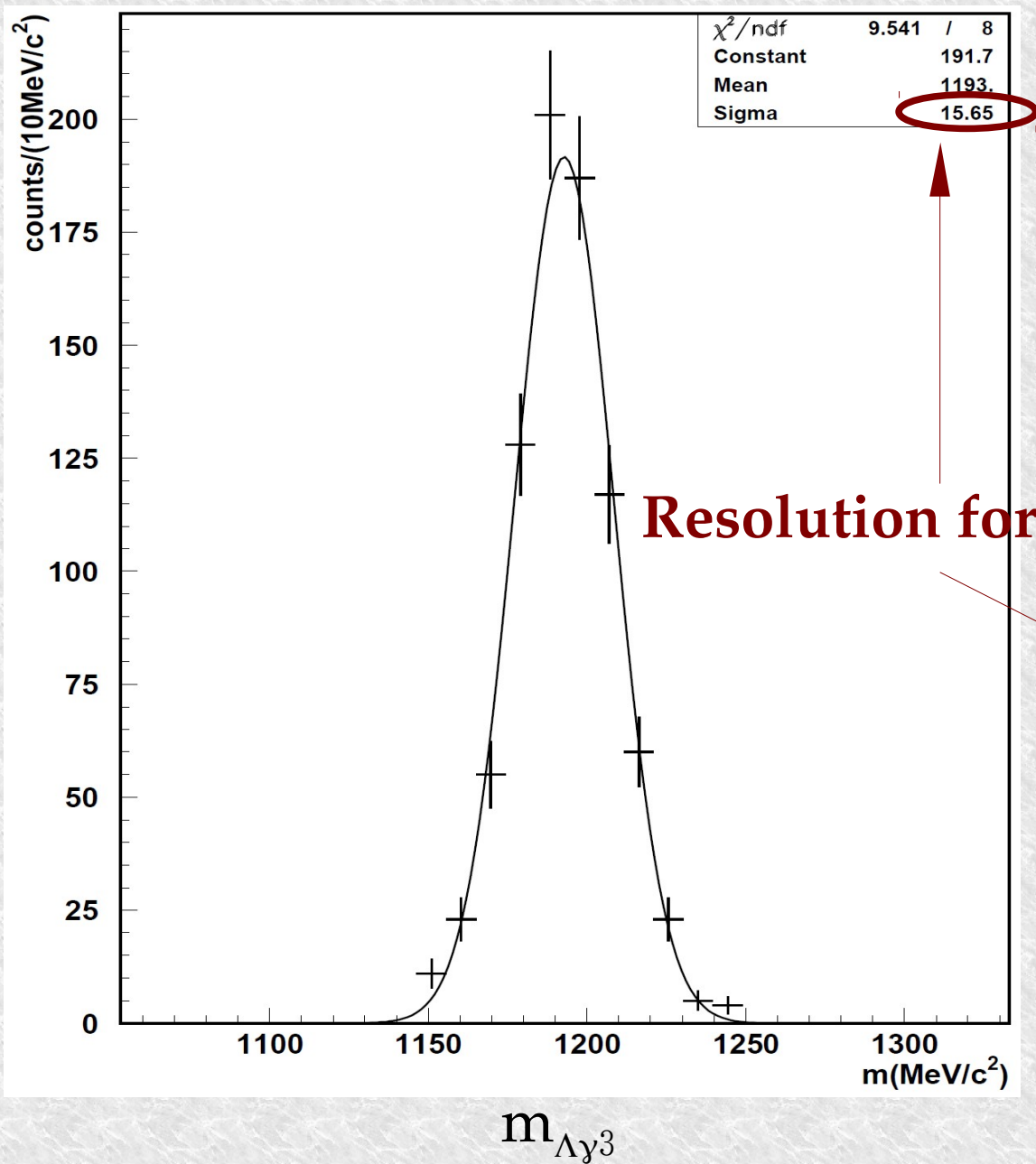
$$\chi_{\pi\Sigma}^2 = \frac{(m_{\pi^0} - m_{ij})^2}{\sigma_{ij}^2} + \frac{(m_{\Sigma^0} - m_{k\Lambda})^2}{\sigma_{k\Lambda}^2}$$

$i, j$  and  $k$  represent one of the previously selected candidate photon cluster.

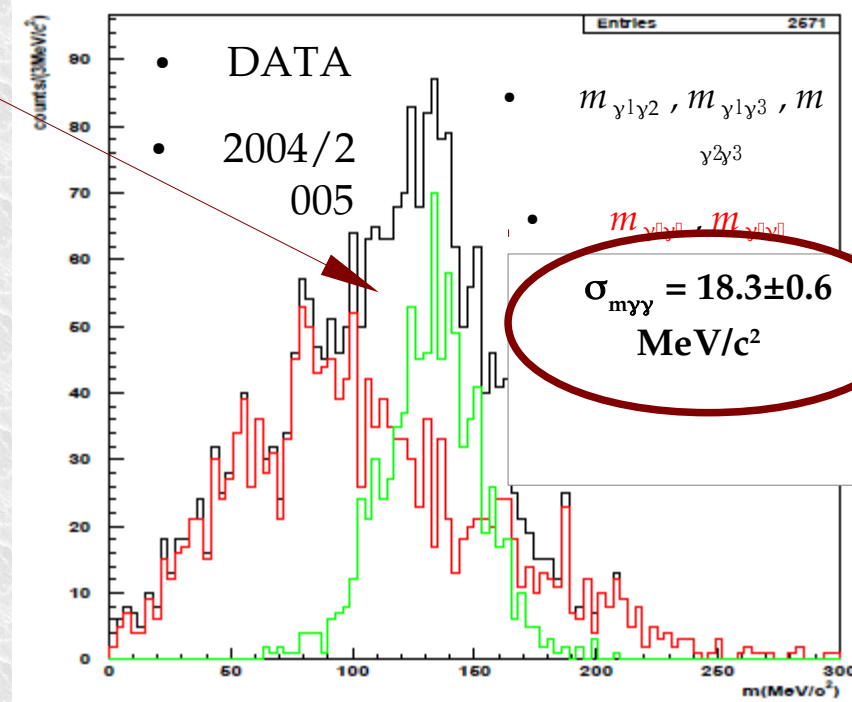
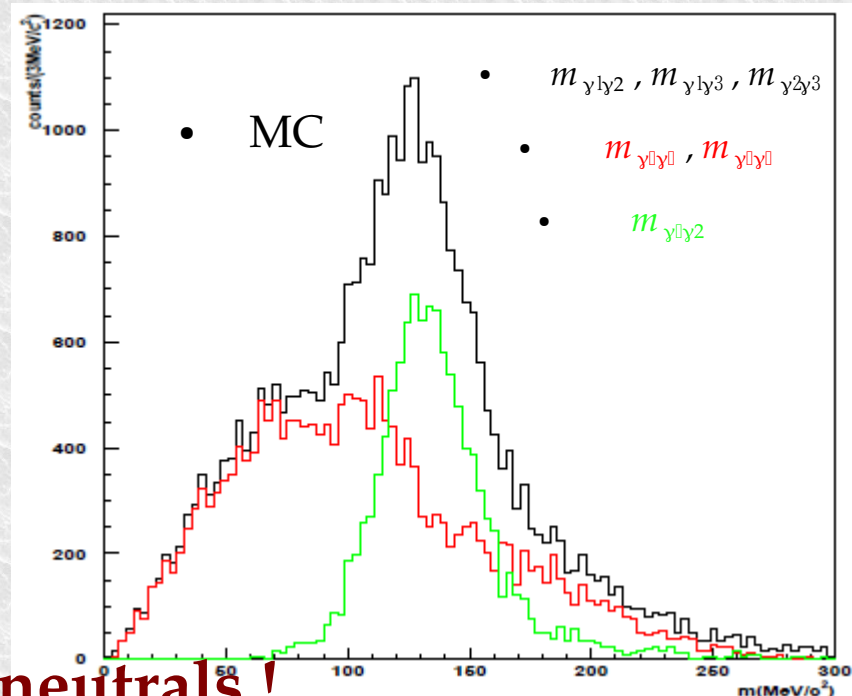
4) Cuts on  $\chi_t^2$  and  $\chi_{\pi\Sigma}^2$  variables were optimized using MC simulations. Specific cuts are introduced in order to avoid the selection of splitted clusters or background for  $\pi^0$

**The algorithm has (from true MC information) an efficiency  $(98\pm 1)\%$  to identify photons and  $(78\pm 2)\%$  to select the correct triple of neutral clusters.**

# Photons selection

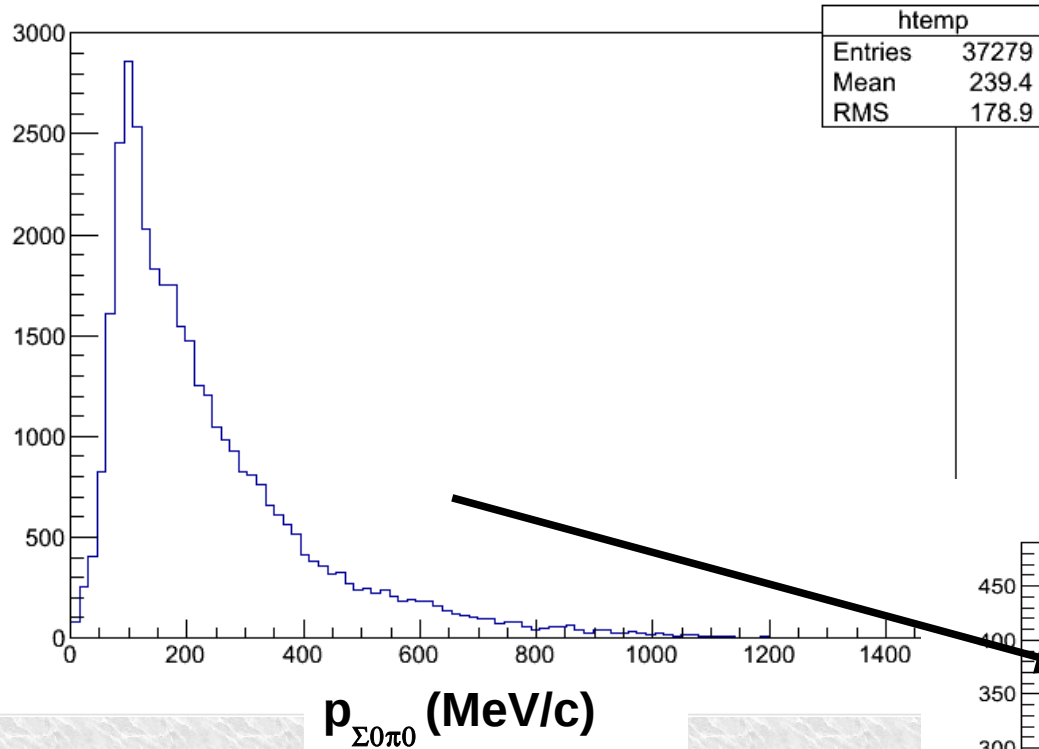


Resolution for neutrals !



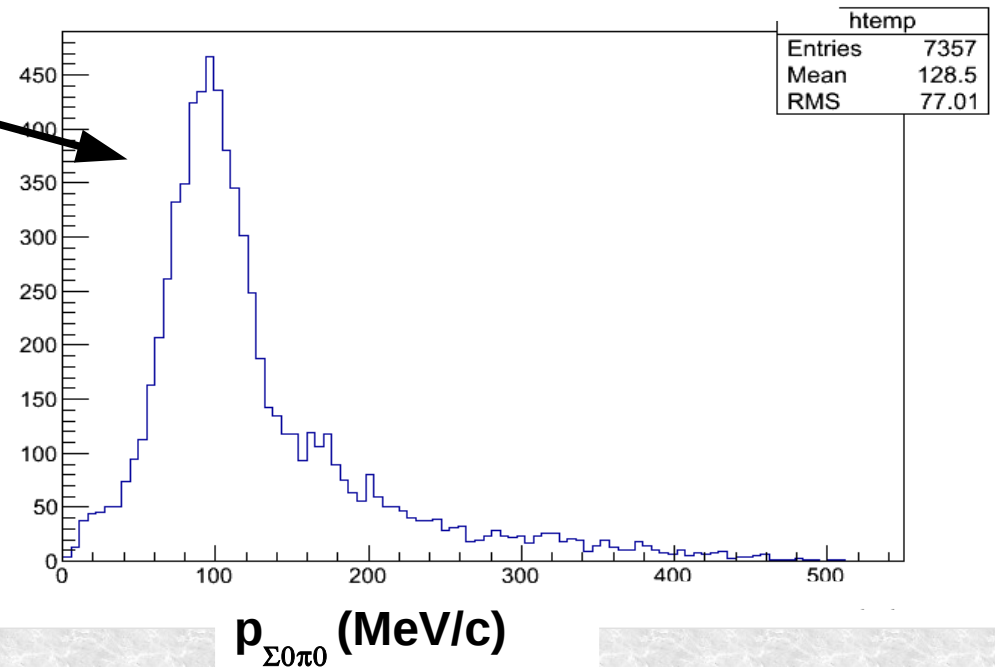


$\Sigma^0\pi^0$  total momentum spectrum clearly shows the  $p_K \sim 100$  MeV/c peak from K- H captures in-flight



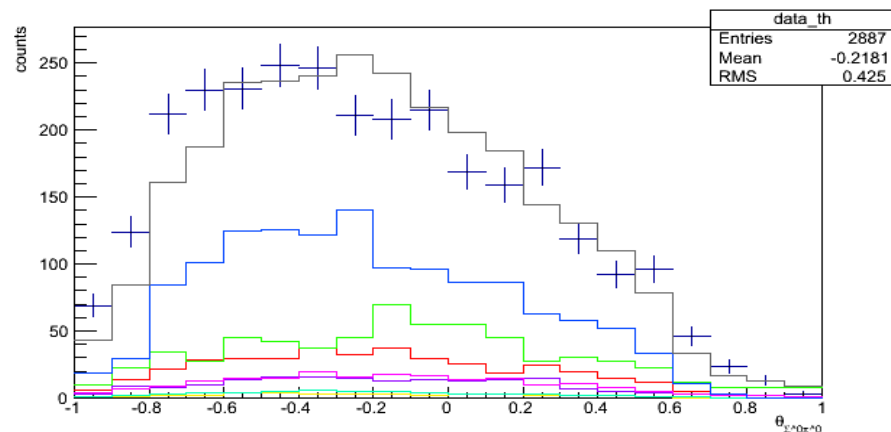
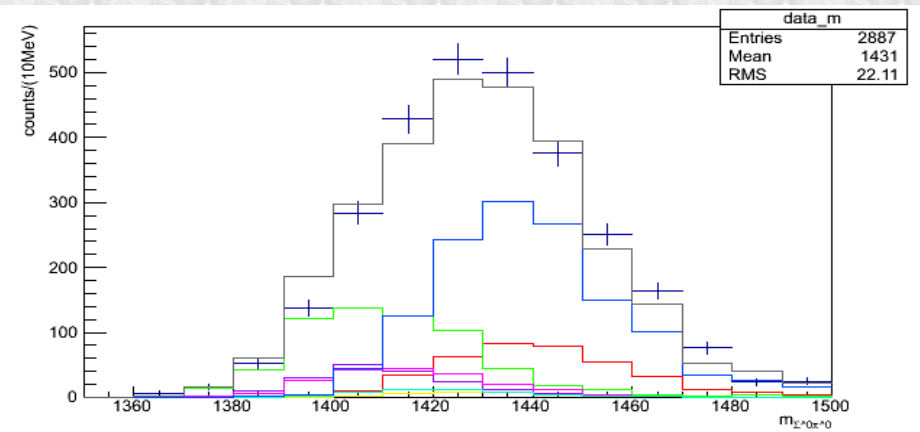
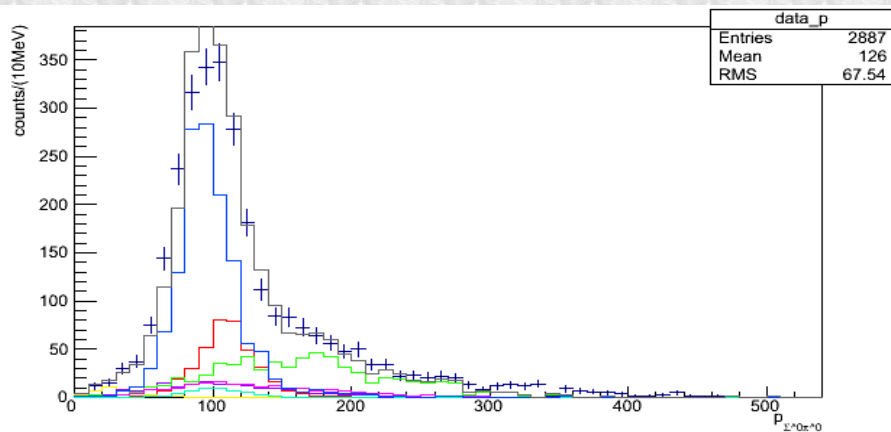
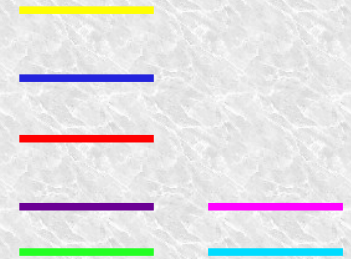
Cuts based on K- H in-flight capture kinematics:

- $\Theta(p_\gamma - p_\gamma) \rightarrow \pi^0$  opening angle
- $p_{\pi^0} \rightarrow \pi^0$  momentum
- $p_{\Sigma^0} \rightarrow \Sigma^0$  momentum



# $K^- p \rightarrow \Sigma^0 \pi^0$ cross section measurement can be done

- K- H capture at-rest  $\rightarrow$  kinematics is closed
- K- H capture in-flight ( $p_K = 90$  MeV)  $\rightarrow$  kinematics is closed
- K- H capture in-flight ( $p_K = 110$  MeV)  $\rightarrow$  kinematics is closed
- K- 4He capture at-rest + in-flight ( $l_K = 1$ )
- K- 12C capture at-rest + in-flight ( $l_K = 2$ , valence proton)



Preliminary